Materials and Methods

Cell culture and reagents

Human lung cancer cells LNM35 [16] and A549 were maintained in RPMI 1640 (Invitrogen, Paisley, UK). All media were supplemented with antibiotics (penicillin 50 U/ml; streptomycin 50 µg/ml) (Invitrogen, Cergy Pontoise; France) and with 10% fetal bovine serum (FBS, Biowest, Nouaille; France). Salinomycin was purchased from Sigma-Aldrich (Sigma-Aldrich, Saint-Quentin Fallavier; France).

Cell viability

Cells were seeded at a density of 5,000 cells/well into 96-well plates. After 24 h, cells were treated for another 24 and 48 h with different concentrations of salinomycin (0.1–50 µM) in triplicate. Control cultures were treated with 0.1% DMSO (the drug vehicle). The effect of salinomycin on cell viability was determined using the CellTiter-Glo Luminescent Cell Viability assay (Promega Corporation, Madison; US), based on quantification of ATP, which signals the presence of metabolically active cells. The luminescent signal was measured using the GLOMAX Luminometer system. Data were presented as proportional viability (%) by comparing the salinomycin-treated cells with the DMSO-treated cells, the viability of which is assumed to be 100%.

Caspase 3/7 activity

Cells were seeded at the density of 5,000 cells/well into 96-well plate and treated with salinomycin (10 and 50 µM) for 24 h, in triplicate. Control cells were exposed to DMSO at a concentration equivalent to that of the salinomycin-treated cells (0.1% DMSO). Caspase-3/7 activity was measured using a luminescent Caspase-Glo 3/7 assay kit following the manufacturer's instructions (Promega Corporation, Madison, USA). Caspase reagent was added and the plate was mixed and incubated for 2.5 h at room temperature. Luminescence was measured using a GLOMAX Luminometer system.

Soft-agar colony growth assay

A layer of agar containing 1 ml of 2.4% low melting temperature Noble agar dissolved in distilled water was poured into wells of a 6-well cell culture dish and allowed to set at 4°C for 5 minutes then incubated at 37°C for 30 min. A second layer (2.9 ml) containing 0.3% of low melting Noble agar dissolved in growth media containing cells (5×10^3 cells/ml) was placed on top of the first layer and allowed to set at 4°C for 5 minutes then transfer them to the humidified incubator at 37°C for 30 minutes to 1 hour. Growth medium (2 ml) was added on top of the second layer and the cells were incubated in a humidified incubator at 37°C for 14 days and then treated for another 7 days with salinomycin (2.5 and 5 µM). Control cells were exposed to 0.1% DMSO. Medium was changed twice a week. At the end of the experiment, colonies were stained for 1 hour with 2% Giemsa stain, and incubated with PBS overnight to remove excess Giemsa stain. The colonies were photographed and scored. Data were presented as proportional colonies (%) by comparing the salinomycin-treated colonies with the DMSO-treated colonies, the colonies of which is assumed to be 100%.

Wound healing motility assay

LNM35 and A549 cells were grown in six-well tissue culture dishes until confluent. Cultures were incubated for 10 min with Moscona buffer. A scrape was made through the confluent monolayer with a plastic pipette tip of 1 mm diameter. Afterwards, the dishes were washed twice and incubated at 37°C in fresh RPMI containing 10% fetal calf serum in the presence or absence of the non-toxic concentrations of salinomycin (0.1–0.5 µM) for A549 and salinomycin (0.05–0.1 µM) for LNM35 cells. Control cells were exposed to 0.1% DMSO. At the bottom side of each dish, two arbitrary places were marked where the width of the wound was measured with an inverted microscope (objective ×4). Motility was expressed as the mean ± SEM of the difference between the measurements at 0, 6, 24 and 30 h after wound.

Matrigel invasion assay

The invasiveness of the lung cancer cells LNM35 treated with salinomycin (0.05–0.1 µM) and A549 cells treated with salinomycin (0.1–0.5 µM) were tested using BD Matrigel Invasion Chambers (8-µm pore size; BD Biosciences, Le Pont de Claix, France) according to manufacturer's protocol. Briefly, cells (1×10^5 cells in 0.5 ml of media and the indicated concentration of salinomycin) were seeded into the upper chambers of the system, the bottom wells in the system were filled with RPMI supplemented with 10% fetal bovine serum as a chemo-attractant and then incubated at 37°C for 24 h. Control cells were exposed to 0.1% DMSO. Non-penetrating cells were removed from the upper surface of the filter with a cotton swab. Cells that have migrated through the Matrigel were fixed with 4% formaldehyde, stained with DAPI and counted in 25 random fields under a microscope. The assay was carried out in duplicate and repeated three times for quantitative analysis. Data were presented as proportional invasiveness (%) by comparing the salinomycin-treated cells with the DMSO-treated cells, the invasion of which is assumed to be 100%.

PCR amplification for NAG-1 mRNA

Isolation of total RNA from cells was performed using a Maxwell 16 Research System (Promega) with a total RNA purification kit (Promega) according to the manufacturer's instructions. The concentration and purity of the RNA samples were determined by measuring the absorbance at 260 nm (A260) and the ratio of the absorbance at 260 nm and 280 nm (ND-1000, NanoDrop Technologies Inc, Wilmington, DE, USA).

Gene Expression analysis was performed using two steps RT-PCR reaction. Firstly Total RNA was converted into cDNA using a High Capacity cDNA Reverse Transcription Kit (Life Technologies, Integrated Gulf Biosystems, Dubai, UAE #4374966) at a final concentration of 50 ng RNA in a 20 µl PCR reaction with 10× RT Buffer 2.0 µl, 25× dNTP Mix (100 mM) 0.8 µl, 10× RT Random Primers 2.0 µl, MultiScribe™ Reverse Transcriptase 1.0 µl, RNase inhibitor 1.0 µl, Nuclease-free water 3.2 µl. Reverse transcription was carried out on a Veriti thermocycler (Life Technologies), using the following parameters: 25°C for 10 min, 37°C for 120 min, and 85°C for 5 min. Quantitative real-time PCR assay for the gene of interest was performed in triplicate on a Fast ABI Prism 7900HT sequence detection system (Life Technologies) using a predesigned Taqman gene expression assay for NAG-1 (GDF15 Life Technologies #Hs00171132_m1) and the Human Hypoxanthine phosphoribosyl transferase (Hprt1 rRNA) as the endogenous control (Life Technologies #4326321E). From the diluted cDNA, 4 µl (20 ng) was used as a template in a 10 µl singleplex PCR reaction containing 2X TaqMan ® Fast Universal PCR Master Mix, No AmpErase ® UNG (5 µl) (Life Technologies #4352042), 20× TaqMan® Gene Expression Assay (0.5 µl), RNase free water 0.5 µl. The PCR thermal cycling parameters were run in Fast mode as follows 50°C for 2 min, 95°C for 20 s followed by 40 cycles of 95°C for 1 s and 60°C for 20 s. Results were initially analyzed with the ABI Prism 7900HT SDS program v2, 4, all remaining calculations and

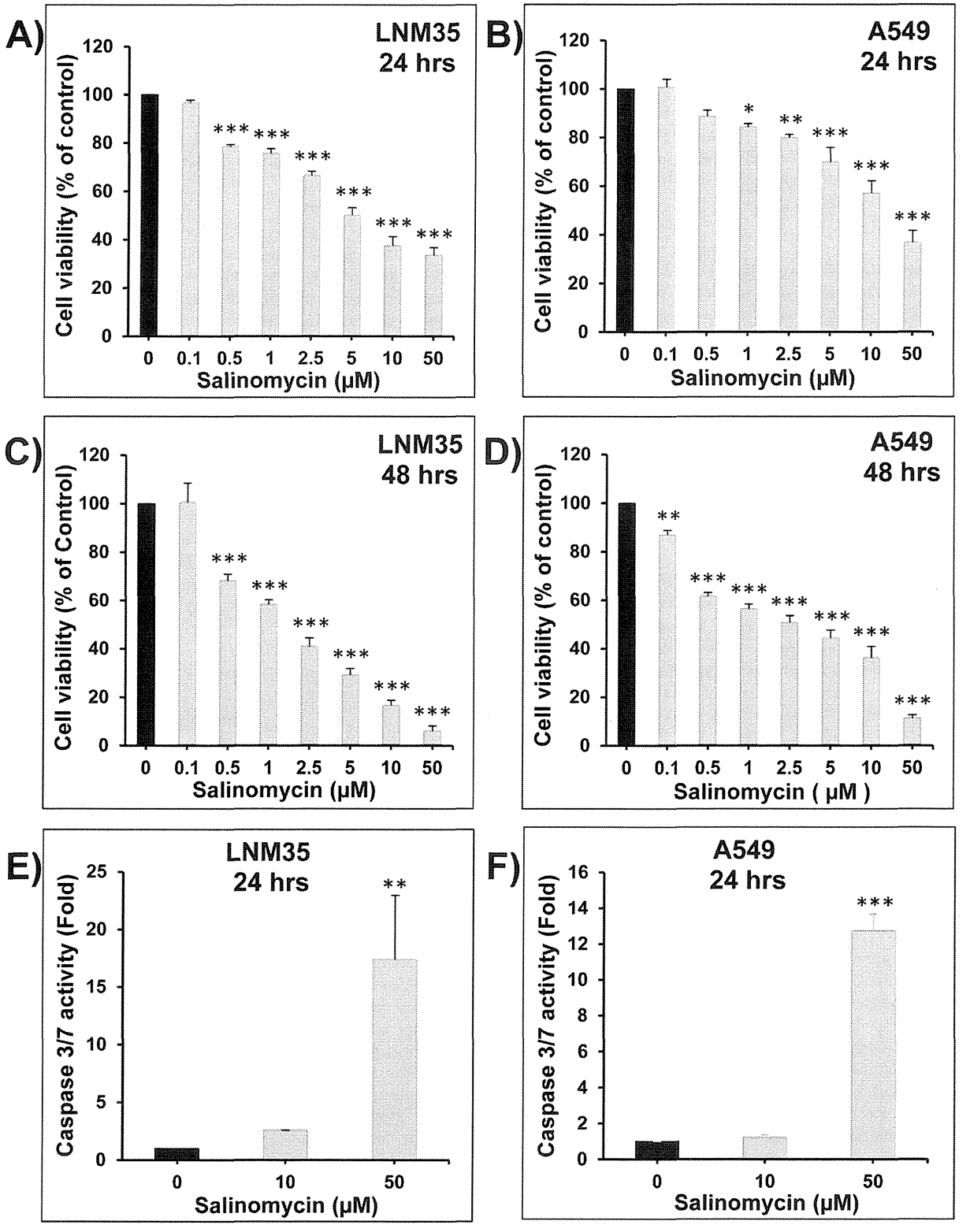

Figure 1. Inhibition of cell viability by salinomycin. Exponentially growing LNM35 (**A, C**) and A549 (**B, D**) cells were treated with vehicle (0.1% DMSO) or the indicated concentrations of salinomycin. The left panel represents 24 h exposure, while the right panel represents 48 h exposure. Viable cells were assayed as described in Materials and Methods. Induction of caspase-3/7 activity was analyzed in LNM35 (**E**) and A549 (**F**) cells treated for 24 h with salinomycin (10 and 50 μM), normalized to the number of viable cells per well and expressed as fold induction compared with the control group. All experiments were repeated at least three times. *Significantly different at $P<0.05$, **Significantly different at $P<0.01$, ***Significantly different at $P<0.001$.

doi:10.1371/journal.pone.0066931.g001

statistical analysis were performed by the SDS RQ Manager 1.1,4 software using the $2-\Delta\Delta Ct$ method with a relative quantification RQmin/RQmax confidence set at 95%

Expression of the pro-apoptotic protein NAG-1

LNM35 and A549 cells were seeded in 100 mm dishes at 3×10^6 cells/dish for 24 h and with increasing concentrations of salinomycin (1–50 μM) for another 24 h. Control cells were exposed to 0.1% DMSO. Total cellular proteins were isolated using RIPA buffer (25 mM Tris.HCl pH 7.6, 1% nonidet P-40, 1% sodium deoxycholate, 0.1% SDS, 0.5% protease inhibitors cocktail, 1% PMSF, 1% phosphatase inhibitor cocktail) from control and treated cells. The whole cell lysate was recovered by centrifugation at 14,000 rpm for 20 minutes at 4°C to remove insoluble material and 30 μg of proteins were separated by SDS-PAGE gel for NAG-1 expression (Cellular Signaling Technology, MA; USA). After electrophoresis, the proteins were transferred on a nitrocellulose membrane, blocked with 5% non-fat milk and probed with NAG-1 (1:200) and β-actin (1:1000) antibodies overnight at 4°C. The blot was washed, exposed to secondary antibodies and visualized using the ECL system (Pierce).

Establishment of stable NAG-1 silencing in lung cancer cells and its impact on the inhibition of cell viability and invasion induced by salinomycin

A549 cells were seeded at a density of 20,000 cells/well into 96-well plates, in the presence of the serum and allowed to attach for 24 h. Cells were transfected with three different designs of SMARTvector 2.0 Lentiviral shRNA particles targeting NAG-1 or SMARTvector 2.0 Non-Targeting control particles (Dharmacon Thermo Scientific, US) that contained a puromycin resistance gene for selection and GFP for identification of positive clones and pools of clones. Selection of cells stably expressing NAG-1 shRNA and the Control shRNA started 72 h post-transfection following the manufacturer's instructions (Dharmacon Thermo Scientific, US). Briefly, growth medium was aspirated from the cells and replaced with fresh selection medium containing 10 μg/mL of puromycin. Puromycin-containing medium was replaced every 2–3days with freshly prepared selection medium, and selection of stable cells expressing NAG1-shRNA or Control shRNA was completed in approximately 4 weeks from commencement of selection. Multiple clones and pools of clones were expanded, and the GFP positive pools of clones were analyzed using western-blot to investigate the expression of NAG-1 following treatment with salinomycin 5 μM. Next, we investigate the invasiveness and the viability of A549 cells expressing NAG1-shRNA or Control shRNA in response to salinomycin.

Statistics

Results were expressed as mean ± S.E.M. of the number of experiments. The difference between experimental and control values were assessed by ANOVA followed by Dunnett's post-hoc multiple comparison test. $P<0.05$ indicate a significant difference.

Results

Salinomycin inhibits lung cancer cell viability

Exposure of LNM35 (**Figure. 1A**) and A549 (**Figure. 1B**) cells to salinomycin concentrations (0.1–50 μM) for 24 or 48 h decreased cell viability in concentration- and time-dependent manner. The IC_{50} concentrations at 24 h were in the range of 5 to 10 μM salinomycin for both cell lines. After 48 h treatment, the IC_{50} concentrations decreased to the range of 1.5 to 2.5 μM salinomycin with 90% inhibition of cell viability in both cells at the concentration of 50 μM.

Activation of caspase-3/7 is essential in apoptotic cell death pathways and was analyzed in LNM35 and A549 cells treated for 24 h with salinomycin (10–50 μM), and normalized to the number of cells per well. Caspase 3/7 activity increased by more than 17-fold in LNM35 cells (**Figure. 1C**) and 12-fold in A549 cells (**Figure. 1D**), following exposure to salinomycin 50 μM. This indicates that salinomycin induce cell death through a caspase 3/7-associated pathway.

Salinomycin impairs colony growth in soft agar

Salinomycin strongly inhibited LNM35 (**Figure. 2A, 2C**) and A549 (**Figure. 2B, 2D**) colony growth in soft-agar in a concentration-dependent manner.

Salinomycin impairs lung cancer cell migration and invasion

Lung cancer patients are at high risk of development of metastasis, starting with cell migration in the primary tumor, leading to local tissue invasion and entry into lymph or blood vessels and finally colonization of distant organs. The ability of salinomycin to reduce cellular migration was investigated using wound-healing model. Salinomycin reduced cellular migration of LNM35 (**Figure. 3A**) and A549 (**Figure. 3B**) cells in a concentration- and time-dependent manner. Similarly, salinomycin impaired the invasion of LNM35 (**Figure. 3C**) and A549 (**Figure. 3D**) cells in the matrigel invasion assay. Salinomycin inhibition of cellular migration and matrigel invasion occurred without significant reduction of cell viability (**Figure. 1**).

Salinomycin induces NAG-1 mRNA and protein expression

First, A549 cells were exposed to different concentrations of salinomycin (0.5–10 μM) for 2 and 24 h total RNA was extracted and evaluated for NAG-1 mRNA expression. As shown in figure 4A, salinomycin induces a marked time- and concentration-dependent induction of NAG-1 mRNA expression with a ten fold increase reached at 24 h after exposure to 10 μM salinomycin (**Figure. 4A**). Next, LNM35 and A549 cells were exposed to different concentrations of salinomycin (1–50 μM) for 24 h and total proteins were evaluated for NAG-1 expression. In both LNM35 and A549 cells, salinomycin induces a marked concentration-dependent induction of NAG-1 protein expression (**Figure. 4B**).

NAG-1 silencing abrogate the anti-invasive effect of salinomycin

As shown in **Figure 5A**, silencing of NAG-1 (NAG-1-shRNA1) reversed the induction of NAG-1 protein expression after treatment with 5 μM of salinomycin. Similar results were obtained with the two other designs of shRNA (NAG-1-shRNA2 and NAG-1-shRNA3) (data not shown). The selectivity of this silencing was confirmed by the fact that no impact on NAG-1 protein expression was observed in the cells transfected with shRNA control particles (control-shRNA) in comparison with the non-transfected cells. Silencing of NAG-1 induction using three different designs of NAG-1-shRNA (1, 2 and 3) failed to decrease the ability of salinomycin to induced A549 cell death (**Figure 5B**), but completely reversed the anti-invasive effect of salinomycin (**Figure 5C**). All together, these results strongly suggest that NAG-1 mediates the anti-invasive, but not the cell death effect of salinomycin.

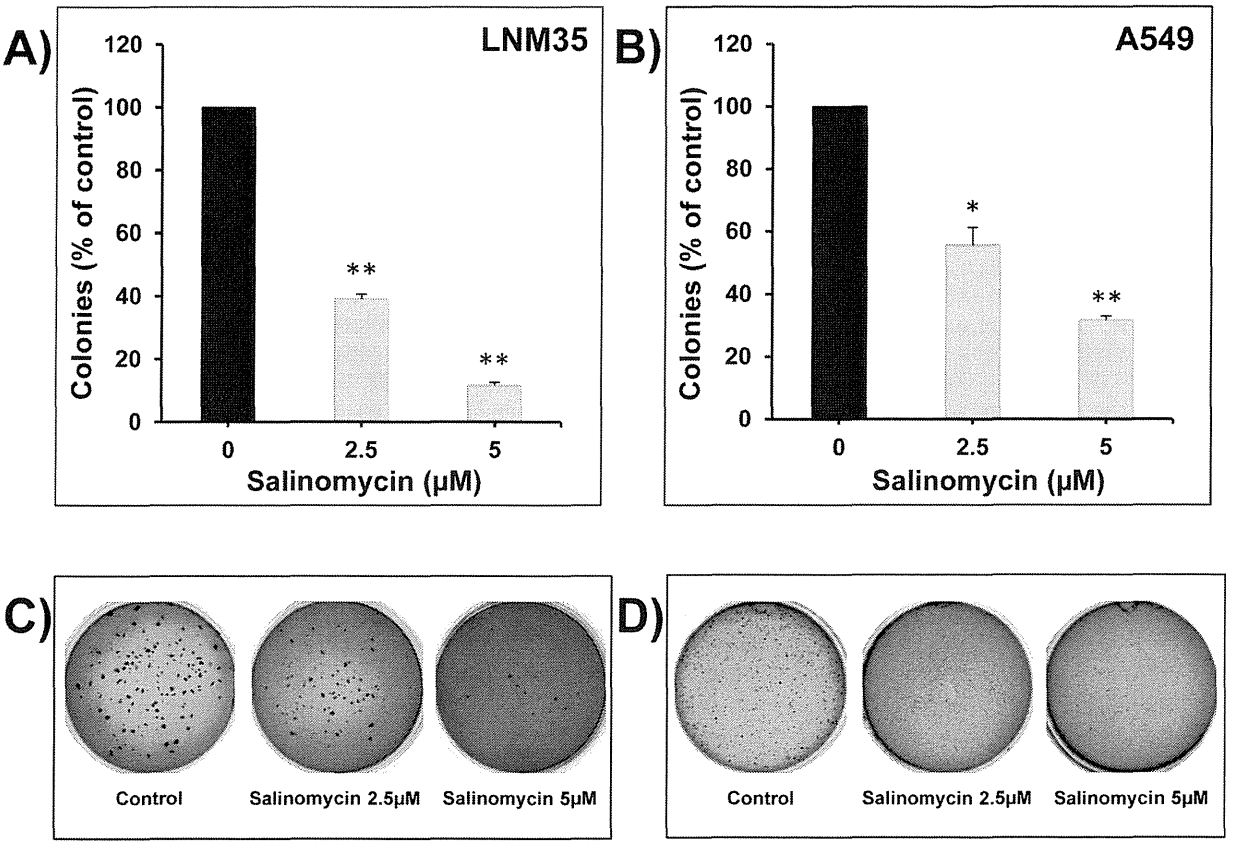

Figure 2. Salinomycin impairs colony growth in soft agar. LNM35 (**A**) and A549 (**B**) cells were grown at a density of 5,000 cells/well in soft agar medium into 6-well plates. After 14 days, formed colonies were treated for 7 days with different concentrations of salinomycin (2.5 and 5 μM). At the end colonies were stained with Giemsa and scored. Representative pictures of the colonies formed in soft agar from LNM35 (**C**) and A549 (**D**) were photographed.
doi:10.1371/journal.pone.0066931.g002

Discussion

Lung cancer is the most common type of cancer worldwide and also has the highest mortality rate. There were 1.61 million cases of lung cancer (12.7% of total cancer burden) in 2008 with 1.38 million deaths (18.2% of all cancer deaths) in the same year [17]. Unfortunately, despite advances in molecular biology of lung cancer, improved diagnosis and even the optimal targeted therapies, the current protocols for the treatment of lung cancer are still insufficient to produce clear and sustained clinical benefits and the cure of lung cancer patients remains unsuccessful. Patients frequently develop resistance to the current targeted therapy drugs and these drugs are also very expensive and not available to the majority of lung cancer patients in the world [18].

In the present study, we investigated the impact of salinomycin on two differentiated human non-small lung cancer cells (LNM35 and A549) survival, colony growth, migration and invasion and the potential role of NAG-1 in the potential anti-cancer effects of salinomycin.

Salinomycin (0.1–50 μM) decreased the viability of LNM35 and A549 differentiated cells in a concentration-, time-dependent and caspase-associated manner. These results are in-line with previously published results showing that low concentrations of salinomycin inhibit the viability of breast cancer stem cells, leukemia stem cells, osteosarcoma stem cells, as well as pancreatic cancer stem cells [8]; [9]; [10]; [11]. During the preparation of this study, another group demonstrated the anticancer activities of salinomycin *in vitro* against the stem cell sub-population in the A549 cells [19]. To confirm this anticancer effect of salinomycin, we investigated its effect on the growth of established colonies. We demonstrated that seven days treatment with low concentration of salinomycin strongly inhibited LNM35 and A549 colony growth in soft agar. These results *in vitro* are in line with other studies demonstrating that salinomycin inhibits breast cancer, osteosarcoma, pancreatic cancer, as well as hepatocellular carcinoma growth in mice [8]; [10]; [11]; [20]. The doses of salinomycin used in these *in vivo* studies were between 4 and 8 mg/kg/I.P which are lower than the LD_{50} dose of salinomycin which was 18 mg/kg intra-peritoneally and 50 mg/kg orally [4]. All together suggest that salinomycin may be a valid and safe anti-cancer agent and further studies will determine the impact of low dose of salinomycin on LNM35 and A549 tumor growth *in vivo* in nude mice.

In the current study, only the highest concentration of salinomycin (50 μM) was able to induce an activation of caspase 3/7 leading to cell death in both lung cancer cells LNM35 and A549. These results are consistent with our recently published work showing that high concentration of salinomycin (50 μM) induced an activation caspase 3/7 and PARP cleavage leading to apoptosis of the breast cancer cells MDA-MB-231 [21]. However, both studies on lung cancer cells and the previously published study on breast cancer cells shows that low concentrations of salinomycin (≤10 μM) resulted more in inhibition of cell proliferation rather than cell death [21]. Similarly, it has been

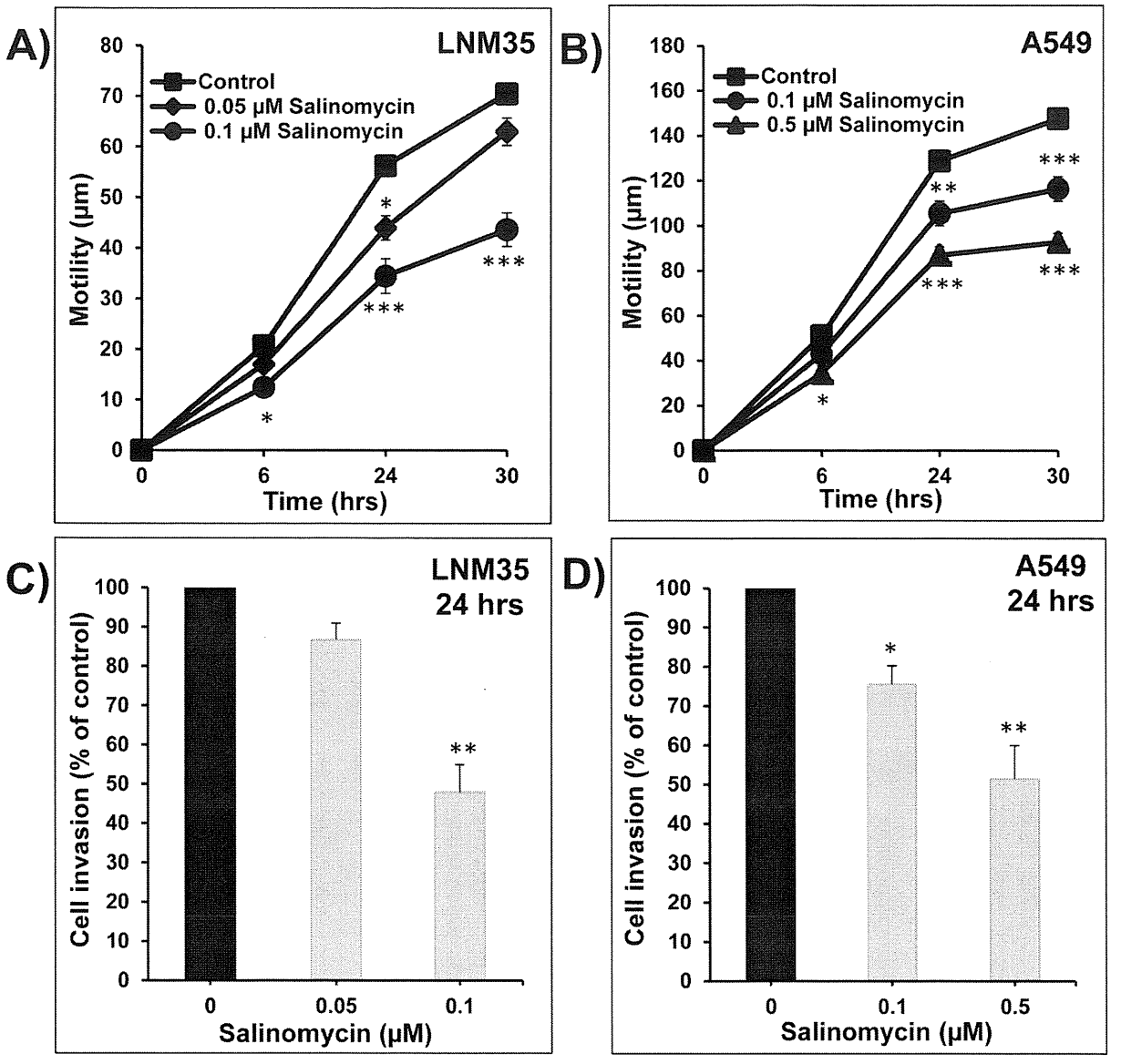

Figure 3. Salinomycin impairs lung cancer cell migration and invasion. Wounds were introduced in LNM35 (**A**) and A549 (**B**) confluent mono-layers cultured in the presence or absence (control) of salinomycin (0.05–0.5 μM). The mean distance that cells travelled from the edge of the scraped area for 6, 24, and 30 h at 37°C was measured in a blinded fashion, using an inverted microscope. **C**) LNM35 cells were incubated for 24 h in the presence or absence of salinomycin (0.05–0.1 μM). **D**) A549 cells were incubated for 24 h in the presence or absence of salinomycin (0.1–0.5 μM). Cells that invaded into Matrigel were scored as described in Materials and Methods.
doi:10.1371/journal.pone.0066931.g003

demonstrated that salinomycin inhibits proliferation and incudes apoptosis of human hepatocellular carcinoma [20].

Cancer progression is associated with abrogation of the normal controls that limits cell migration and invasion, eventually leading to metastasis. Since metastases are the major cause of death in cancer patients, the development of new treatment regimens that reduce invasion and metastasis is highly important for cancer therapy. In this context, we demonstrated that salinomycin induced a highly significant time- and concentration-dependent inhibition of cell migration and invasion *in vitro* of the two differentiated lung cancer cell lines LNM35 and A549. These results are in agreement with previous studies showing that salinomycin selectively inhibits breast cancer stem cells metastases *in vivo* [8] and prostate cancer cell migration *in vitro* [22].

The anti-cancer molecular mechanism of action of salinomycin has been investigated in several studies. In this context, it has been demonstrated that salinomycin is an effective anticancer agent that induced apoptosis in human cancer cells independent of tumor suppressor protein p53 and caspases activation [9]. These results are in agreement with our recent study showing that salinomycin significantly decreased viability of the wild-type p53 MCF-7 and T47D as well as mutant p53 MDA-MB-231 and T47D human breast cancer cell lines in time- and concentration-dependent manners [21]. It was also shown that salinomycin triggers apoptosis of PC3 prostate cancer cells by elevating the intracellular ROS level, leading to the translocation of Bax protein to mitochondria, cytochrome c release, activation of the caspase-3, and cleavage of PARP [23]. Salinomycin also induces caspase dependent cell-death in RKO, SW480 and SW620 colon cancer

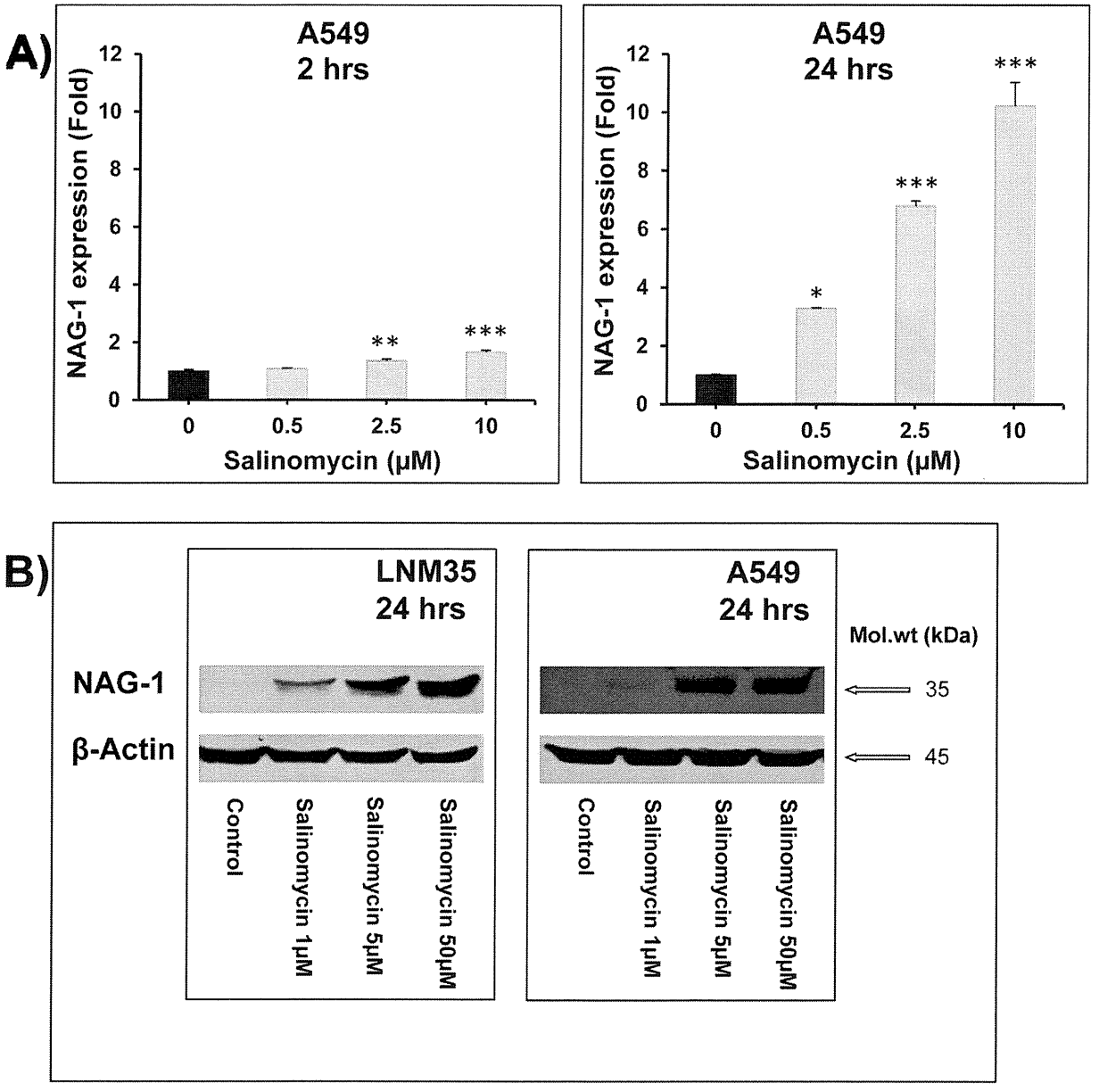

Figure 4. Induction of NAG-1 expression by salinomycin. Cells were exposed to different concentrations of salinomycin, and total RNA was extracted after 2 and 24 hours and analyzed for NAG-1 mRNA expression in A549 cells (**A**) and after 24 h for protein expression in both A549 and LNM35 cells (**B**).
doi:10.1371/journal.pone.0066931.g004

cells [24]. It has also been demonstrated that salinomycin is an effective inhibitor of osteosarcoma stem cells as well as lymphocytic leukemia cells partially through down-regulation of the Wnt/μ-catenin self-renewal pathway [10]; [20]; [25]. Another study showed that salinomycin inhibited prostate cancer cell growth by reducing aldehyde dehydrogenase and nuclear factor-μB activities [22]. Similarly, it has been demonstrated that salinomycin inhibits Akt/NF-κB pathway leading to apoptosis in cisplatin resistant ovarian cancer cells [26]. It has also been demonstrated that salinomycin induces autophagy in colon and breast cancer cells [24]. Increased phosphorylation of the DNA damage-related proteins (e.g. pH2AX, p53BP1, pBRCA1, pChk1) proteins indicates greater DNA breakage and damage [27]. Salinomycin increases DNA strand breaks and induces phosphorylation of the DNA damage-related protein, H2AX [28].

The NSAID-activated gene (NAG-1, GDF-15, and MIC-1) is induced by several apoptosis-inducing agents in colon, prostate, and lung cancer cells [15]; [29]. NAG-1 was involved in the synergistic induction of apoptosis by combined treatment of sodium salicylate and PI3K/MEK1/2 inhibitors in A549 human lung adenocarcinoma cells [30]. The NAG-1 expression levels substantially increase in cancer cells, serum, and/or cerebrospinal fluid during the progression of diverse human aggressive cancers, such as intracranial brain tumors, melanoma, gastrointestinal, pancreatic, colorectal, prostate, breast, and lung epithelial cancers. Of clinical interest, an enhanced NAG-1 expression has been

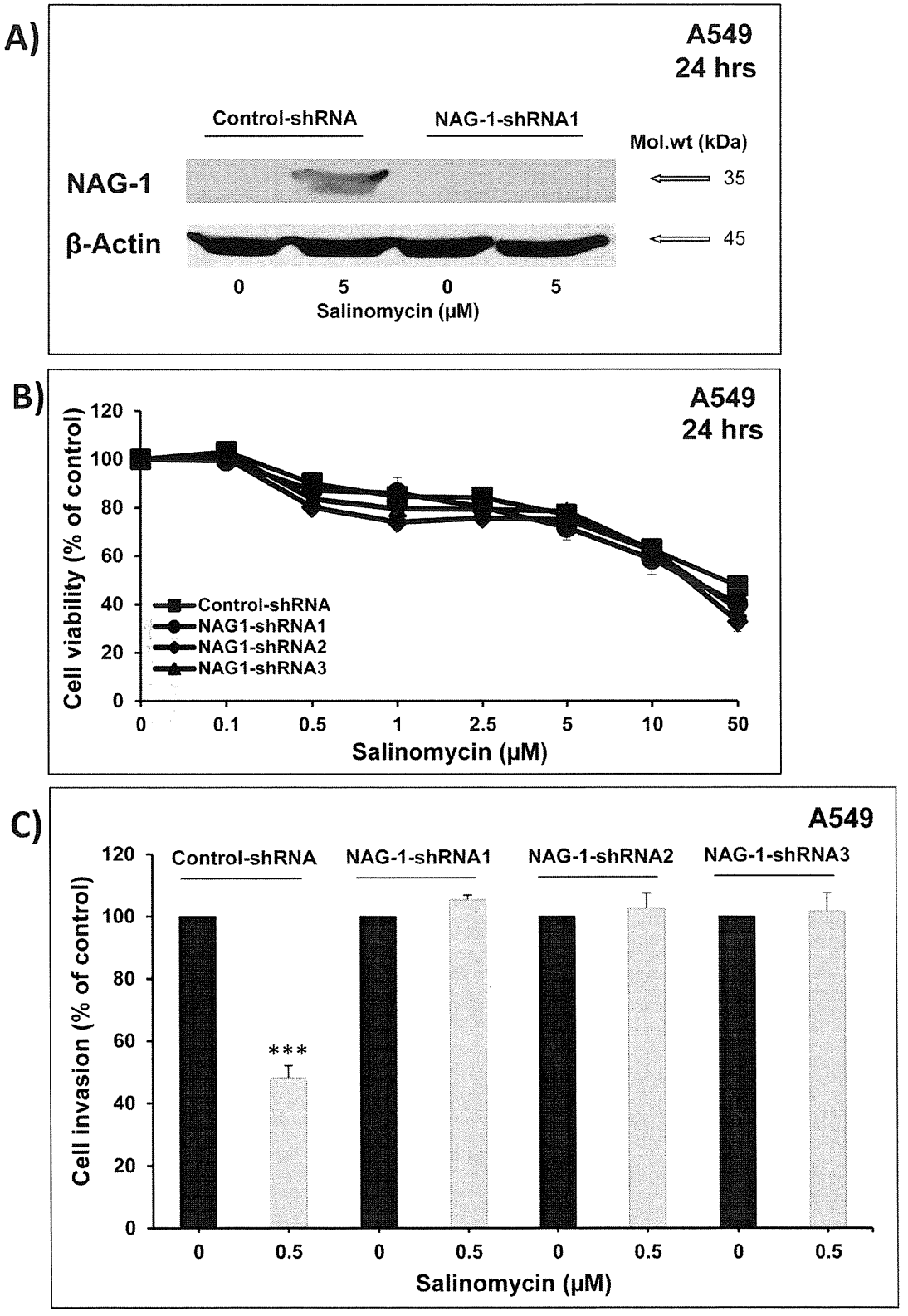

Figure 5. The induction of NAG-1 expression by salinomycin mediate its anti-invasive potential. Silencing of NAG-1 suppressed the increased expression of NAG-1 induced by salinomycin (**A**) without impact on the inhibition of the A549 cell viability induced by salinomycin (**B**) leading to complete suppression on anti-invasive potential of salinomycin (**C**).
doi:10.1371/journal.pone.0066931.g005

positively correlated with poor prognosis and patient survival [29]; [30]; [31]; [32].

We hypothesized that NAG-1 is involved in the anti-cancer effects of salinomycin and we demonstrated for the first time that salinomycin induced a clear time- and concentration-dependent induction of NAG-1 expression. We also clearly demonstrated that NAG-1 contributes to the inhibition of lung cancer cell invasion but not to the induction of cell death, mediated by salinomycin. In contrast, it has been reported that NAG-1 expression was associated with a more invasive gastric cancer cell line phenotype and could induce increased gastric cancer cell invasion *in vitro* [33].

It has been demonstrated that salinomycin improve the efficacy of gemcitabine to eradicate pancreatic cancer [11]. Salinomycin also sensitizes breast cancer cells to the effects of doxorubicin and etoposide treatment by increasing DNA damage [28]. In the same context, the combination therapy of octreotide modified paclitaxel active targeting micelles and salinomycin passive targeting micelles improve the treatment of breast cancers through the eradication of breast cancer cells together with breast cancer stem cells [34]. Similarly, the combination therapy of trastuzumab and salinomycin was superior to single treatment with each drug in the treatment of HER2-positive breast cancer cells as well as breast cancer stem cells [35]. We recently reported *in vitro*, that salinomycin was also able to potentiate the anticancer effects of the 4-Hydroxytamoxifen and the frondoside A on breast cancer cells MCF-7 and MDA-MB-231 respectively [21]. Building on these aforementioned results, and knowing from clinical trials that single agent treatments rarely result in clinical benefits to cancer patients, and that combination therapies are in usual necessary for effective treatment of tumors, we investigated the therapeutic advantage of combination of cisplatin, (a first line therapeutic for lung cancer), with salinomycin in both LNM35 and A549 cells. Unfortunately, we found that cisplatin was not able to enhance the inhibition of lung tumor cell viability induced by salinomycin (Attoub et al, Unpublished data).

The current finding identifies salinomycin as a promising novel therapeutic agent not only for the depletion of cancer stem cells but also for the differentiated lung tumors.

Acknowledgments

We thank Dr. Katarina Hostanska from Institute for Complementary Medicine; University Hospital Zurich, Switzerland for providing the A549 cells.

Author Contributions

Conceived and designed the experiments: SA TA. Performed the experiments: KA RI YA KP. Analyzed the data: SA KA TA KP. Contributed reagents/materials/analysis tools: SA TA RI TT. Wrote the paper: SA TA.

References

1. Dempke WC, Suto T, Reck M (2010) Targeted therapies for non-small cell lung cancer. Lung Cancer 67: 257–274.
2. Spira A, Ettinger DS (2004) Multidisciplinary management of lung cancer. N Engl J Med 350: 379–392.
3. Korpanty G, Smyth E, Carney DN (2011) Update on anti-angiogenic therapy in non-small cell lung cancer: Are we making progress? J Thorac Dis 3: 19–29.
4. Miyazaki Y, Shibuya M, Sugawara H, Kawaguchi O, Hirsoe C (1974) Salinomycin, a new polyether antibiotic. J Antibiot (Tokyo) 27: 814–821.
5. Mahmoudi N, de Julián-Ortiz JV, Ciceron L, Gálvez J, Mazier D, et al. (2006) Identification of new antimalarial drugs by linear discriminant analysis and topological virtual screening. J Antimicrob Chemother 57: 489–497.
6. Naujokat C, Fuchs D, Opelz G (2010) Salinomycin in cancer: A new mission for an old agent. Mol Med Report 3: 555–559.
7. Huczynski A (2012) Salinomycin: a new cancer drug candidate. Chem Biol Drug Des 79: 235–238.
8. Gupta PB, Onder TT, Jiang G, Tao K, Kuperwasser C, et al. (2009) Identification of selective inhibitors of cancer stem cells by high-throughput screening. Cell 138: 645–659.
9. Fuchs D, Heinold A, Opelz G, Daniel V, Naujokat C (2009) Salinomycin induces apoptosis and overcomes apoptosis resistance in human cancer cells. Biochem Biophys Res Commun 390: 743–749.
10. Tang QL, Zhao ZQ, Li JC, Liang Y, Yin JQ, et al. (2011) Salinomycin inhibits osteosarcoma by targeting its tumor stem cells. Cancer Lett 311: 113–121.
11. Zhang GN, Liang Y, Zhou LJ, Chen SP, Chen G, et al. (2011) Combination of salinomycin and gemcitabine eliminates pancreatic cancer cells. Cancer Lett 313: 137–144.
12. Bauskin AR, Brown DA, Kuffner T, Johnen H, Luo XW, et al. (2006) Role of macrophage inhibitory cytokine-1 in tumorigenesis and diagnosis of cancer. Cancer Res 66: 4983–4986.
13. Liu T, Bauskin AR, Zaunders J, Brown DA, Pankhurst S, et al. (2003) Macrophage inhibitory cytokine 1 reduces cell adhesion and induces apoptosis in prostate cancer cells. Cancer Res 63: 5034–5040.
14. Golkar L, Ding XZ, Ujiki MB, Salabat MR, Kelly DL, et al. (2007) Resveratrol inhibits pancreatic cancer cell proliferation through transcriptional induction of macrophage inhibitory cytokine-1. J Surg Res 138: 163–169.
15. Breit SN, Johnen H, Cook AD, Tsai VW, Mohammad MG, et al. (2011) The TGF-β superfamily cytokine, MIC-1/GDF15: a pleotrophic cytokine with roles in inflammation, cancer and metabolism. Growth Factors 29: 187–195.
16. Kozaki K, Miyaishi O, Tsukamoto T, Tatematsu Y, Hida T, et al. (2000) Establishment and characterization of a human lung cancer cell line NCI-H460-LNM35 with consistent lymphogenous metastasis via both subcutaneous and orthotopic propagation. Cancer Res 60: 2535–2540.
17. Ferlay J, Shin HR, Bray F, Forman D, Mathers C, et al. (2010) Estimates of worldwide burden of cancer in 2008: GLOBOCAN 2008. Int J Cancer 12: 2893–2917.
18. Hait WN (2010) Anticancer drug development: the grand challenges. Nat Rev Drug Discov 9: 253–254.
19. Wang Y (2011) Effects of salinomycin on cancer stem cell in human lung adenocarcinoma A549 cells. Med Chem 7: 106–111.
20. Wang F, He L, Dai WQ, Xu YP, Wu D, et al. (2012) Salinomycin inhibits proliferation and induces apoptosis of human hepatocellular carcinoma cells in vitro and in vivo. PLoS One 7: e50638.
21. Al Dhaheri Y, Attoub S, Arafat K, Abuqamar S, Eid A, et al. (2013) Salinomycin induces apoptosis and senescence in breast cancer: upregulation of p21, downregulation of survivin and histone H3 and H4 hyperacetylation. Biochim Biophys Acta 1830: 3121–3135.
22. Ketola K, Hilvo M, Hyötyläinen T, Vuoristo A, Ruskeepää AL, et al. (2012) Salinomycin inhibits prostate cancer growth and migration via induction of oxidative stress. Br J Cancer 106: 99–106.
23. Kim KY, Yu SN, Lee SY, Chun SS, Choi YL, et al. (2011) Salinomycin-induced apoptosis of human prostate cancer cells due to accumulated reactive oxygen species and mitochondrial membrane depolarization. Biochem Biophys Res Commun 413: 80–86.
24. Verdoodt B, Vogt M, Schmitz I, Liffers ST, Tannapfel A, et al. (2012) Salinomycin induces autophagy in colon and breast cancer cells with concomitant generation of reactive oxygen species. PLoS One 7: e44132.
25. Lu D, Choi MY, Yu J, Castro JE, Kipps TJ, et al. (2011) Salinomycin inhibits Wnt signaling and selectively induces apoptosis in chronic lymphocytic leukemia cells. Proc Natl Acad Sci U S A 108: 13253–13257.
26. Parajuli B, Lee HG, Kwon SH, Cha SD, Shin SJ, et al. (2013) Salinomycin inhibits Akt/NF-κB and induces apoptosis in cisplatin resistant ovarian cancer cells. Cancer Epidemiol.
27. Solier S, Sordet O, Kohn KW, Pommier Y (2009) Death receptor-induced activation of the Chk2- and histone H2AX-associated DNA damage response pathways. Mol Cell Biol 29: 68–82.
28. Kim JH, Chae M, Kim WK, Kim YJ, Kang HS, et al. (2011) Salinomycin sensitizes cancer cells to the effects of doxorubicin and etoposide treatment by increasing DNA damage and reducing p21 protein. Br J Pharmacol 162: 773–784.
29. Mimeault M, Batra SK (2010) Divergent molecular mechanisms underlying the pleiotropic functions of macrophage inhibitory cytokine-1 in cancer. J Cell Physiol 224: 626–635.
30. Kim CH, Kim MY, Moon JY, Hwang JW, Lee SY, et al. (2008) Implication of NAG-1 in synergistic induction of apoptosis by combined treatment of sodium salicylate and PI3K/MEK1/2 inhibitors in A549 human lung adenocarcinoma cells. Biochem Pharmacol 75: 1751–1760.
31. Kadara H, Schroeder CP, Lotan D, Pisano C, Lotan R (2006) Induction of GDF-15/NAG-1/MIC-1 in human lung carcinoma cells by retinoid-related molecules and assessment of its role in apoptosis. Cancer Biol Ther 5: 518–522.
32. Yu YL, Su KJ, Chen CJ, Wei CW, Lin CJ, et al. (2012) Synergistic anti-tumor activity of isochaihulactone and paclitaxel on human lung cancer cells. J Cell Physiol 227: 213–222.
33. Lee DH, Yang Y, Lee SJ, Kim KY, Koo TH, et al. (2003) Macrophage inhibitory cytokine-1 induces the invasiveness of gastric cancer cells by up-

regulating the urokinase-type plasminogen activator system. Cancer Res 63: 4648–4655.
34. Zhang Y, Zhang H, Wang X, Wang J, Zhang X, et al. (2012) The eradication of breast cancer and cancer stem cells using octreotide modified paclitaxel active targeting micelles and salinomycin passive targeting micelles. Biomaterials 33: 679–691.
35. Oak PS, Kopp F, Thakur C, Ellwart JW, Rapp UR, et al. (2012) Combinatorial treatment of mammospheres with trastuzumab and salinomycin efficiently targets HER2-positive cancer cells and cancer stem cells. Int J Cancer 12: 2808–2819.

PLOS ONE

Met Is the Most Frequently Amplified Gene in Endometriosis-Associated Ovarian Clear Cell Adenocarcinoma and Correlates with Worsened Prognosis

Yoriko Yamashita[1,2]*, Shinya Akatsuka[1], Kanako Shinjo[1,3], Yasushi Yatabe[4], Hiroharu Kobayashi[1,3], Hiroshi Seko[1], Hiroaki Kajiyama[3], Fumitaka Kikkawa[3], Takashi Takahashi[5], Shinya Toyokuni[1]

1 Department of Pathology and Biological Responses, Nagoya University Graduate School of Medicine, Nagoya, Aichi, Japan, **2** Department of Pathology, Nagoya City University Hospital, Nagoya, Aichi, Japan, **3** Department of Obstetrics and Gynecology, Nagoya University Graduate School of Medicine, Nagoya, Aichi, Japan, **4** Department of Pathology and Molecular Diagnostics, Aichi Cancer Center Hospital, Nagoya, Aichi, Japan, **5** Division of Molecular Carcinogenesis, Center for Neurological Diseases and Cancer, Nagoya University Graduate School of Medicine, Nagoya, Aichi, Japan

Abstract

Clear cell adenocarcinoma of the ovary (OCC) is a chemo-resistant tumor with a relatively poor prognosis and is frequently associated with endometriosis. Although it is assumed that oxidative stress plays some role in the malignant transformation of this tumor, the characteristic molecular events leading to carcinogenesis remain unknown. In this study, an array-based comparative genomic hybridization (CGH) analysis revealed Met gene amplification in 4/13 OCC primary tumors and 2/8 OCC cell lines. Amplification of the AKT2 gene, which is a downstream component of the Met/PI3K signaling pathway, was also observed in 5/21 samples by array-based CGH analysis. In one patient, both the Met and AKT2 genes were amplified. These findings were confirmed using fluorescence *in situ* hybridization, real-time quantitative PCR, immunoblotting, and immunohistochemistry. In total, 73 OCC cases were evaluated using real-time quantitative PCR; 37.0% demonstrated Met gene amplification (>4 copies), and 8.2% had AKT2 amplification. Furthermore, stage 1 and 2 patients with Met gene amplification had significantly worse survival than patients without Met gene amplification ($p<0.05$). Met knockdown by shRNA resulted in reduced viability of OCC cells with Met amplification due to increased apoptosis and cellular senescence, suggesting that the Met signaling pathway plays an important role in OCC carcinogenesis. Thus, we believe that targeted inhibition of the Met pathway may be a promising treatment for OCC.

Citation: Yamashita Y, Akatsuka S, Shinjo K, Yatabe Y, Kobayashi H, et al. (2013) Met Is the Most Frequently Amplified Gene in Endometriosis-Associated Ovarian Clear Cell Adenocarcinoma and Correlates with Worsened Prognosis. PLoS ONE 8(3): e57724. doi:10.1371/journal.pone.0057724

Editor: Junji Yodoi, Institute for Virus Research, Laboratory of Infection and Prevention, Japan

Received September 10, 2012; **Accepted** January 25, 2013; **Published** March 4, 2013

Funding: This study was supported by a Grant-in-Aid from the Japan Society of the Promotion of Science, Tokyo, Japan. The funders had no role in study design, data collection and analysis, decision to publish, or preparation of the manuscript.

Competing Interests: The authors have declared that no competing interests exist.

* E-mail: k46581a@nucc.cc.nagoya-u.ac.jp

Introduction

Clear cell adenocarcinoma of the ovary (OCC) is frequently associated with endometriosis [1], and the existence of abundant free iron in endometriotic cysts due to hemorrhage is proposed as a cause of persistent oxidative stress and subsequent carcinogenesis [2]. Oxidative stress due to iron overload causes genomic amplification in ferric nitrilotriacetate (Fe-NTA)-induced rat carcinoma cells [3], and the genomic changes observed in these animals are specific, showing close similarity to human tumors [4]. OCC is a chemo-resistant tumor with a relatively poor prognosis [5], and recent reports suggest that specific molecular events such as an activating mutation of the alpha-catalytic domain of PI3 kinase (PI3K) [6] or an inactivating mutation of AT-rich interactive domain 1A (ARID1A) [7,8] may play roles in the tumorigenesis of OCC. However, focusing on genomic copy number change analyses, multiple studies performed by different groups using either comparative genomic hybridization (CGH) or array-based CGH analysis in OCC cases have failed to demonstrate specific gene amplification [9–11]. Recently, a study from the United Kingdom reported Her2 amplification at chromosome 17q12 in 14% of the investigated OCC cases using array-based CGH analysis [12], emphasizing the molecular heterogeneity of the tumor. Using double in situ hybridization (DISH) and immunohistochemistry, Yamamoto et al also reported Met amplification in 28% of Japanese OCC cases [13]. Most recently, another report from Japan demonstrated that ZNF217 at chromosome 20q13.2 was amplified in 20% of OCC patients [14]. In this study, we performed an array-based CGH analysis using Japanese OCC samples and detected genomic amplification of the Met gene in 6/21 samples. Additionally, we determined that the Met gene was the most frequently amplified gene in these samples. We also detected amplification of the AKT2 gene, which is one of the three isoforms of AKT kinase, a downstream component of the Met/PI3K signaling pathway. This is the first study to report the frequent amplification of a specific gene in OCC detected by array-based CGH analysis

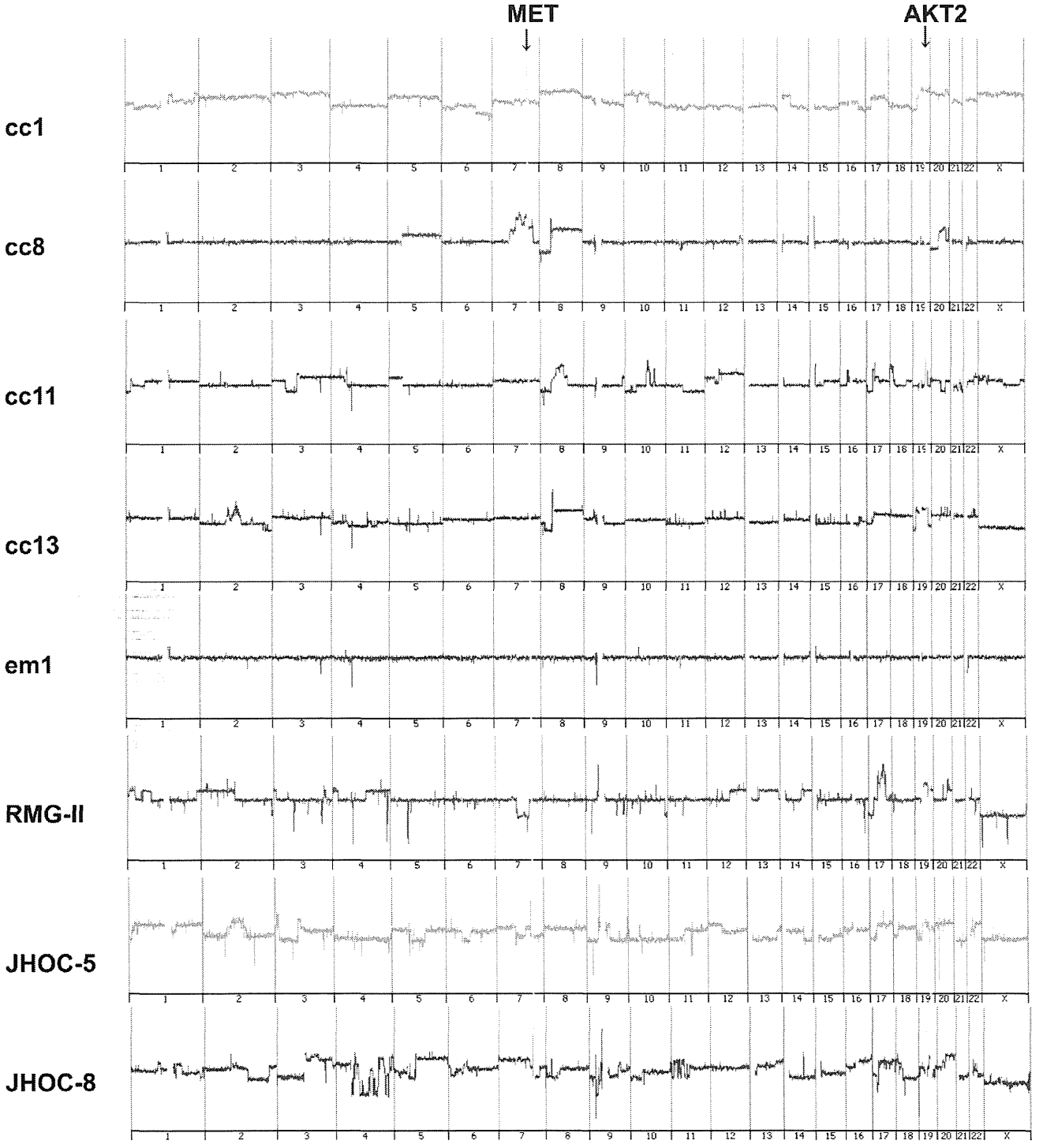

Figure 1. Representative array-based CGH analysis data of chromosomes 1–22 and X. The data of 4 ovarian clear cell adenocarcinoma samples (cc1, cc8, cc11, cc13), 1 endometrioid adenocarcinoma sample (em1), and 3 cell lines (RMG-II, JHOC-5, and JHOC-8) are shown. Met amplification is observed in cc1, cc8, and cc13 and JHOC-5 and JHOC-8 cells. AKT2 amplification is observed in cc11 and cc13 and JHOC-8 and RMG-II cells.
doi:10.1371/journal.pone.0057724.g001

and the first to report AKT2 amplification in OCC. We further analyzed a larger number of OCC samples in knockdown experiments to investigate the role of the Met/PI3K/AKT pathway in OCC tumorigenesis.

Materials and Methods

Patients and Samples

Formalin-fixed, paraffin-embedded tissues from 73 ovarian clear cell carcinoma patients and 3 ovarian endometrial adenocarcinoma patients at Nagoya University Hospital were obtained

with written informed consent. Microscopically negative lymph node samples without metastasis were also obtained from the patients for use as controls. The experimental designs of the genomic and expression studies were reviewed and approved by the Committee for Bioethics of Nagoya University Graduate School of Medicine (#671).

Cell Lines

ES-2, KOC-7C, RMG-II, and TOV21G were cultured with RPMI-1640 (Sigma) with 10% FBS. JHOC-5, JHOC-7, JHOC-8, and JHOC-9 cells were provided from Riken BRC, Tsukuba, Japan, and were cultured with DMEM/F12 (Sigma)-based medium, according to the distributor's instructions.

Array-based Comparative Genomic Hybridization

Genomic DNA was isolated and labeled using the Oligonucleotide Array-Based CGH for Genomic DNA Analysis (ULS labeling) Kit (Agilent Technologies, Santa Clara, CA, USA), according to the manufacturer's instructions. Briefly, 4 continuous 5 μm paraffin-sections were placed in an Eppendorf tube, and after paraffin removal and proteinase K treatment, genomic DNA was extracted using the DNeasy Blood & Tissue Kit (Qiagen, Valencia, CA, USA) with modifications. After 5 minutes of heat fragmentation at 95°C, reference DNA from the lymph node samples was labeled with Cy3, and tumor DNA was labeled with Cy5. The two samples were then mixed together after the removal of residual unlabeled fluorescent dye and then hybridized to a Human Genome CGH 244A Oligo Microarray (G4411B, Agilent Technologies). After washing, stabilization, and drying, the microarrays were scanned with an Agilent Scanner (Agilent) and analyzed with DNA Analytics Software (ver. 4.0) (Agilent). Genomic DNA was obtained from cell lines and control early passage immortalized human female B cells [15] for copy number reference and then applied to the array-based CGH analysis as previously described [16].

Fluorescence *In Situ* Hybridization

Bacterial artificial chromosome clones (RP11-95I20 and RP11-163C9 for the Met gene) were selected from http://genome.ucsc.edu/and purchased from http://bacpac.chori.org/. DNA was then extracted by the NucleoBond PC 20 Plasmid DNA Purification Kit (Macherey-Nagel, Düren, Germany) with modifications.

Fluorescent probes were labeled by incorporating Green-dUTP (Vysis; Abbott Laboratories; Abbott Park, IL, USA) into the DNA using the Nick Translation Kit (Vysis). CEP 7 (D7Z1) Spectrum Orange Probe (Vysis) was purchased as a control probe. Fluorescence *in situ* hybridization (FISH) was performed using the probes, Paraffin Pretreatment Kit, and LSI/WCP Hybridization Buffer (Vysis) according to the manufacturer's protocol. Briefly, paraffin sections were treated with protease, and after denaturation, the probes were hybridized to nuclear DNA, counterstained with DAPI, and visualized using a fluorescence microscope.

Real-time Quantitative PCR

A total of 50 ng of isolated genomic DNA was applied per reaction for real-time quantitative PCR (qPCR). Sample DNA was amplified for 40 cycles with an annealing temperature of 55°C using the TaqMan Universal PCR Kit (ABI) and 7300 Real-time PCR System (ABI) following the manufacturer's instructions. The sequences of the primers and internal probes were as follows: Met (sense), 5′-TCCTGGGCACCGAAAGG-3′; Met (antisense), 5′-GAGGCGAGGGATTGGGTACT-3′; Met reporter probe, 5′-FAM-CAGCCCCTTTCAGATC-MGB-3′. For the AKT2 gene, a TaqMan Copy Number Assay Kit for AKT2 (Hs00113634; ABI) including the FAM/MGB-labeled AKT2 probe was used. VIC-TAMRA-labeled TaqMan Copy Number Reference (TERT) primers and probes (ABI) were used as controls for both assays. PCR products were quantified in triplicate and normalized to the human TERT gene using the Delta-delta Ct method according to the manufacturer. To compare the relative amount of AKT isoform expression, a quantitative reverse transcription PCR (qRT-PCR) analysis was performed using plasmids encoding the PCR products of AKT1 or AKT2 using the following primers: AKT1 (sense) 5′-CCCAAGCACGCGTGACCAT-3′; AKT1 (antisense) 5′-GCGTAGTAGCGGCCTGTGGC-3′; AKT2 (sense) 5′-GAGGTCATGGAGCACAGGTT-3′; AKT2 (antisense) 5′-CTGGTCCAGCTCCAGTAAGC-3′.

PCR products (100–200 bp) were subcloned into the pGEM-TEasy vector (Promega, Madison, WI) by TA-cloning according to the manufacturer's instructions, and the plasmids were then used as control templates to establish standard curves. Then, qRT-PCR analyses were performed to detect AKT1 or AKT2 as previously described [17].

Immunoblotting and Immunohistochemistry

The primary antibodies against human c-Met, AKT1, AKT2, and phosphorylated-AKT (Ser473) were clones 3D4 (Invitrogen, Carlsbad, CA, USA), D26, C7H310, D6G4, and 736E11 (Cell Signaling Technologies, Danvers, MA, USA), respectively. Western blotting and immunohistochemical staining were performed as previously described [15,17]. The established scoring criteria were used for immunohistochemical staining as follows:

2+: more than 50% positive tumor cells with strong intensity in the cell membrane.

1+: less than 50% positive tumor cells with strong intensity in the cell membrane or more than 50% but weak staining in the tumor cell membrane or any intensity staining without tumor cell membrane staining.

- : no staining.

Retroviral and Lentiviral Transduction of Short-hairpin RNA

The construction of short-hairpin RNA (shRNA)-encoding retroviral vectors were performed as previously described [15]. Briefly, the precursor form of shRNA was ligated into an entry vector encoding the human H1 promoter and then transferred to the destination vectors by the Gateway system (Invitrogen). The lentiviral vectors pCS-RfA-CG, pCAG-HIVgp, and pCMV-VSV-G-RSV-Rev were obtained from Dr. Miyoshi's lab (Riken BRC, Tsukuba, Japan). After transfer of the H1 promoter and shRNA precursor, shRNA-encoding lentiviruses were produced by the transient transfection of 3 plasmids into 293T cells, and the harvested viral particles were subsequently used for target cell transduction in nearly the same manner as the retroviruses described above. The sense-coding sequences of the shRNA were as follows: shMet 2, GCAGTGAATTAGTTCGCTA; shMet5, GGGAATCATCATGAAAGAT; shNC, ATCTGAAGACCTATTTTAT.

Cell Growth and Survival Assays

OCC cell lines (JHOC-5, JHOC-8, and ES-2) and control HeLa cells were transiently transfected by Met-shRNA- or control

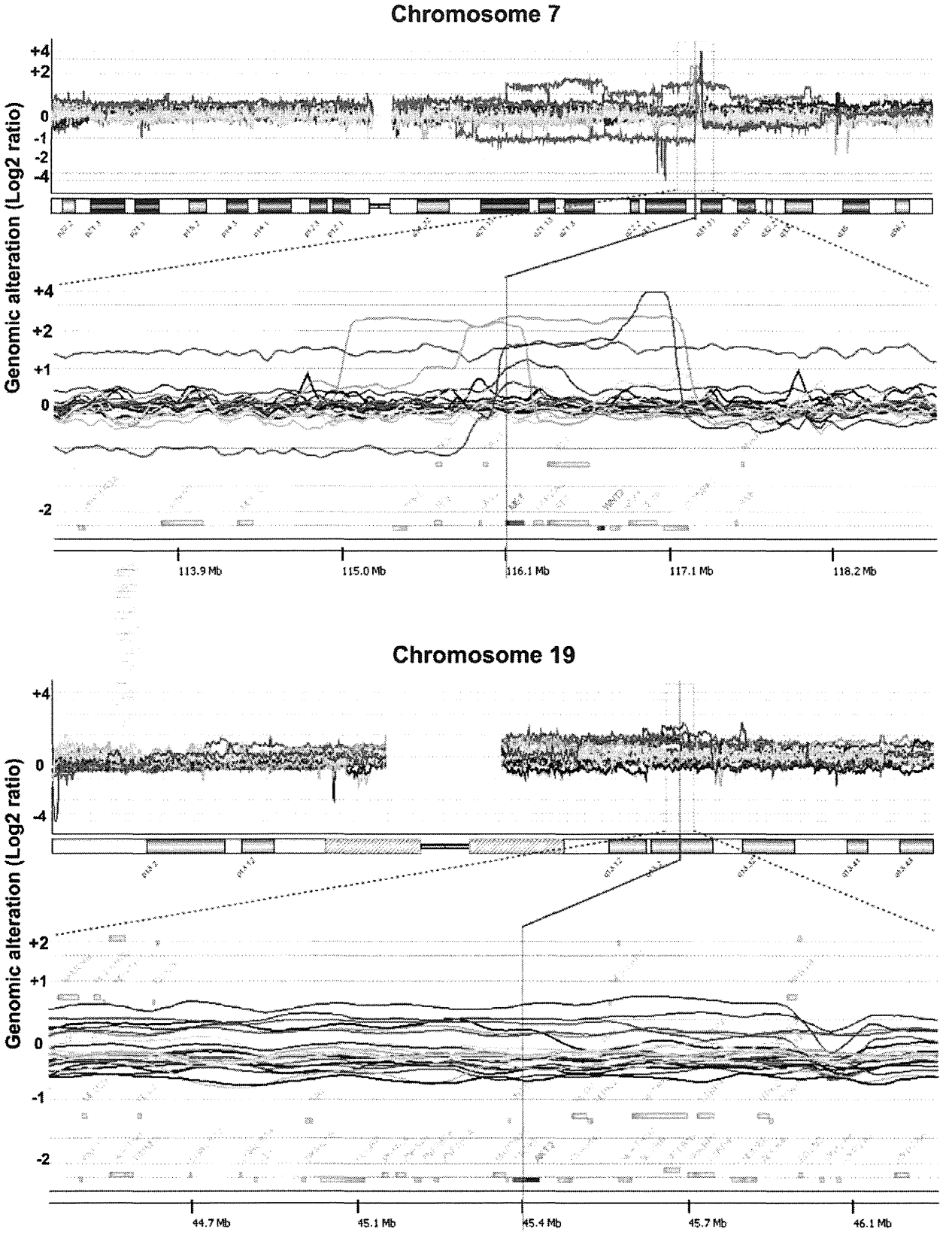

Figure 2. Gene and chromosome views of the amplified regions in array-based CGH analysis. Genomic changes in the 21 ovarian clear cell adenocarcinoma samples are shown. High, clear peaks within 2 Mb are observed in 6/21 samples at the genomic region encoding Met (upper row). The amplified region including AKT2 is also shown (lower row).
doi:10.1371/journal.pone.0057724.g002

Table 1. Summary of the histological features and genomic changes in samples applied to the array-based comparative genomic hybridization.

	Histologic Features			Met Immunostaining	Met		AKT2		Other aCGH Characteristics	
Sample	Cysts	Hemorrhage or Hemosiderin Deposits	Endometriosis		aCGH	qPCR	aCGH	qPCR	p16 copy no.	PTEN copy no.
cc1	+	+	+	++	+++	5.4		<2	nc	nc
cc2	+	+	+	++	++	2.1		<2	nc	nc
cc3	+	+	+	+		<1.5		<2	nc	nc
cc4	+	+	−	+		<1.5		<2	nc	nc
cc5	+	+	+	+		<1.5	++	2.6	nc	nc
cc6	−	−	−	+		<1.5		<2	nc	nc
cc7	+	+	+	+		<1.5		<2	nc	nc
cc8	+	+	+	++	++	3.6		<2	nc	nc
cc9	+	+	+	+		<1.5		<2	nc	nc
cc10	+	+	+	+		<1.5		<2	nc	nc
cc11	+	+	+	+		<1.5	++	3.2	nc	nc
cc12	+	+	+	+		<1.5		<2	nc	nc
cc13	+	+	−	++	+	1.6	++	2.6	nc	nc
em1	+	+	−	−		<1.5		<2	nc	nc
em2	+	−	+	+		<1.5		<2	nc	nc
em3	+	−	−	−		<1.5		<2	nc	nc

aCGH: array-based comparative genomic hybridization, qPCR: real-time quantitative PCR, nc: no change.
doi:10.1371/journal.pone.0057724.t001

shRNA-coding retroviral vectors described above. Cells were transferred to chamber slides after 24 hours. At day 2 post-transfection, cells were fixed with neutralized 4% formalin and then subjected to a TdT-mediated dUTP-biotin nick end labeling (TUNEL) assay and a senescence assay using the ApopTag Plus Peroxidase In Situ Apoptosis Detection Kit (Chemicon International, Temecula CA, USA) and Senescence Detection Kit (BioVision Research Products, Mountain View, CA, USA), respectively. To estimate the numbers of viable cells, cells were transferred to 96-well plates 24 hours after transfection. At day 4 post-transfection, 250 μl of 0.4 mg/ml thiazolyl blue tetrazolium bromide (MTT) was added to each well and incubated for 1 hour at 37°C. After removal of the solution, 100 μl of dimethylsulfoxide was added to each well and incubated for 10 minutes at room temperature. Finally, the absorbance due to formazan formation was determined at 570 nm.

Statistical Analyses

Student's t-test was used to analyze the MTT assay results. A Kaplan-Meier analysis was performed with the log-rank test using SPSS (IBM) software version 17.0.

Results

Array-based Comparative Genomic Hybridization Analysis

Of the 73 OCC cases, DNA extracted from 13 tumors and 3 endometrioid adenocarcinoma samples was subjected to array-based CGH analysis. The genomic gains of the chromosome 7q31.31 region were frequently less than 2 Mb in length, showing peaks at the area of the Met oncogene, and were detected in 4 of the 13 OCC cases (cc1, cc2, cc8, cc13) (**Figs. 1 and 2**). Frequent amplification of the 19q3.2 region including the AKT2 gene with a smaller peak (less than 1 Mb) was also observed in 3 of the 13 cases (cc5, cc11, cc13). One case (cc13) had amplification of both genes (i.e., Met and AKT2). We then performed an array-based CGH analysis of 8 OCC cell lines and detected amplification of the Met gene in 2: JHOC-5 and JHOC-8. The other 134 genomic regions amplified in more than 20% of the 21 samples, including 13 primary tumors and 8 cell lines, are shown in **Table S1**. The genes other than Met and AKT2 with previously known functions positively affecting cell growth were Lyn, P-Rex2, Jag2, Map3K10, and Bcl3 (shown in red in **Table S1**), but the significance of the genes included in other amplified segments remains unclear. No amplification or deletion was observed in the CDKN2A region of chromosome 9 or the PTEN-encoding region of chromosome 10. Met amplification was not observed in any of the three endometrioid adenocarcinoma samples, and the genomic changes were rather inconspicuous compared to the clear cell carcinoma samples (**Figs. 1 and 2**). Summarizing the array-based CGH results, the copy number aberration analysis revealed that chromosomes 8q, 19q, 1q, and 20q had a relatively high frequency of genome gain, and chromosome 8p, 19p, and 17p tended to have genome loss (**Fig. S1**). The clinical, histological, and genetic data of the 13 OCC cases and 3 endometrioid adenocarcinoma cases used in the array-based CGH analyses are summarized in **Table 1**.

Confirmation of Met Amplification

We then confirmed amplification of the Met gene by FISH (**Fig. 3**). A centromere probe of chromosome 7 (CEP7) was used as a reference to count the amplification signals. All 4 samples that showed Met amplification by array-based CGH analysis had an increased Met/CEP 7 ratio, confirming the results of the array-based CGH analysis. We further confirmed the Met gene copy number increase by real-time quantitative PCR. Using the

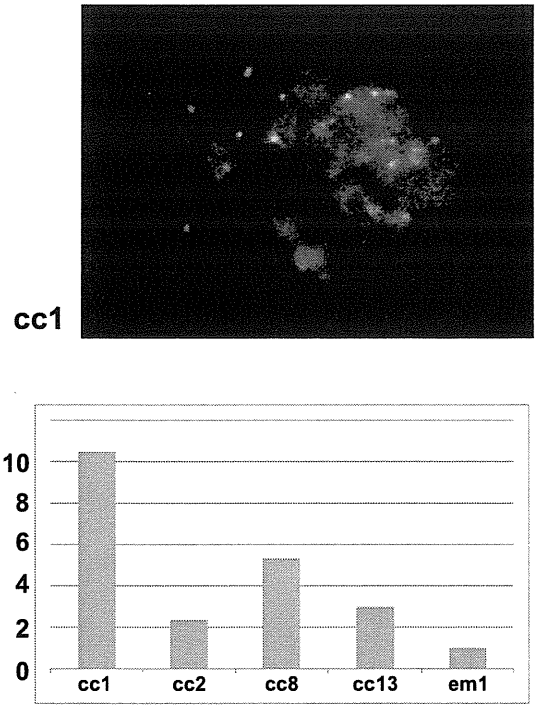

Figure 3. FISH analysis for confirmation of Met amplification. A representative nucleus of a Met-amplified cell (cc1) is shown in the upper figure (Green: Met probe, Orange: CEP 7; centromere 7 probe, Blue; DAPI). The lower graph shows the FISH signal number (MET/CEP 7 ratio) of the 4 Met-amplified ovarian clear cell adenocarcinoma samples (cc1, cc2, cc8, cc13) and an endometrioid adenocarcinoma case (em1) without Met amplification. A total of 60 cells were counted for each sample, average numbers (Met: CEP7) were as follows; cc1(18:2.0), cc2(4.4:2.1),cc8(10:2.2), cc13(4.6/1.7), em1(1.7/1.9). All values were then normalized with that of em1 as 1.0.
doi:10.1371/journal.pone.0057724.g003

hTERT copy number reference as a control, we successfully demonstrated that all 4 Met-amplified samples and none of the 9 samples without Met amplification showed more than a 1.5-fold increase in DNA quantity (**Fig. 4A**). We further confirmed Met amplification in the cell lines by real-time quantitative PCR (**Fig. 4B**), which also showed good correlation with the array-based CGH analysis. To confirm that the protein level change accompanied gene alteration, we performed Western blotting using the 8 OCC cell lines (**Fig. 5A**). The total amount of Met protein was clearly increased in JHOC-5 and JHOC-8 cells, both of which demonstrated Met genome amplification. Immunostaining of 13 OCC samples also revealed overexpression of the Met protein in the gene-amplified samples (**Fig. 5B** and **Table 1**). Thus, we found Met gene amplification in 6 of the 21 OCC samples (28.5%) analyzed by array-based CGH analysis, all of which were confirmed by qPCR and protein expression analyses.

Confirmation of AKT2 Amplification

We next confirmed the AKT2 gene copy number increase by qPCR and demonstrated that all three AKT2-amplified samples and none of the ten samples without Met amplification showed more than a 1.5-fold increase in DNA quantity (**Fig. 4C**). Amplification of the AKT2 gene was detected in two cell lines, namely, RMG-II and JHOC-8, by array-based CGH analysis (**Figs. 1 and 2**) and was also confirmed by real-time quantitative PCR (**Fig. 4D**). Western blotting using the 8 OCC cell lines revealed that both AKT1 and AKT2 were highly expressed in

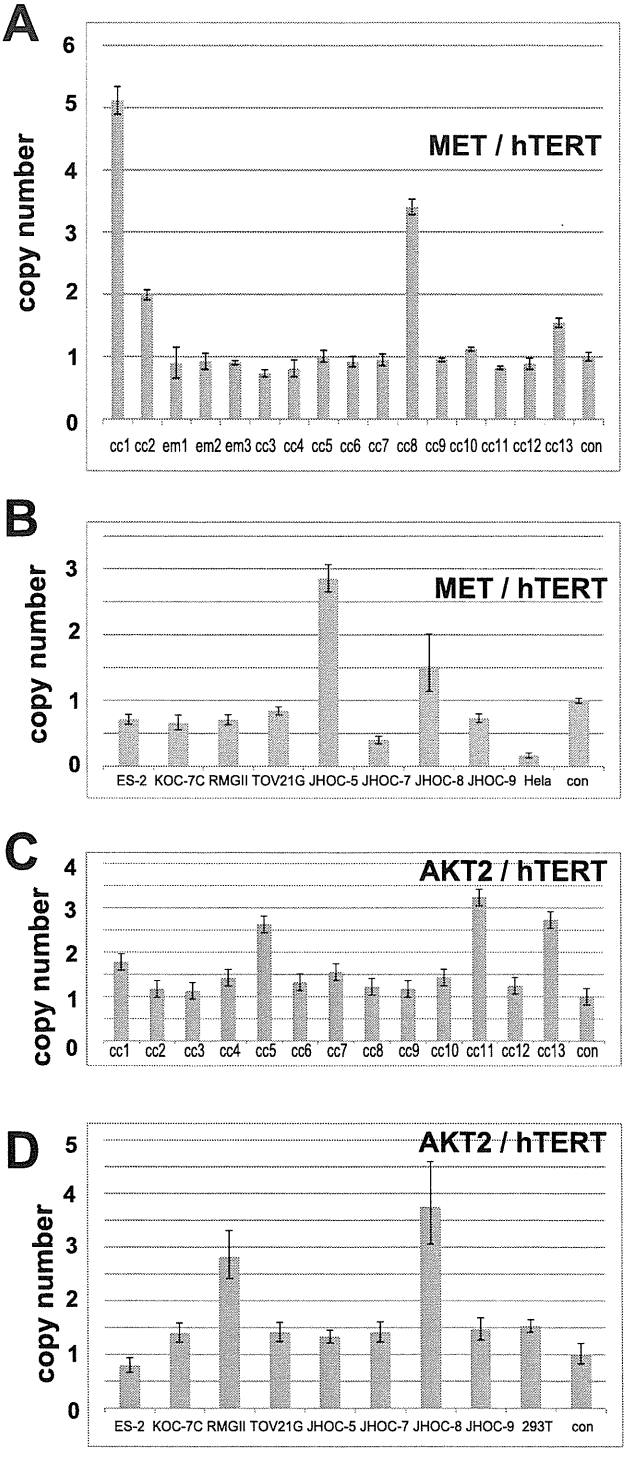

Figure 4. QPCR confirmation of Met and AKT2 amplification. A. Copy number change analysis of Met in 13 ovarian clear cell adenocarcinoma samples are shown. Four samples (cc1, cc2, cc8, cc13) had a Met/hTERT ratio greater than 1.5. **B.** Copy number change analysis of Met in 8 ovarian clear cell adenocarcinoma cell lines are shown. Two cell lines (JHOC-5 and JHOC-8) had a Met/hTERT ratio greater than 1.5. **C.** Copy number change analysis of AKT2 in 13 ovarian clear cell adenocarcinoma samples are shown. Three samples (cc5, cc11, cc13) had an AKT2/hTERT ratio greater than 1.5. **D.** The qPCR results for the copy number change analysis of AKT2 in 8 ovarian clear cell adenocarcinoma cell lines are shown. Two cell lines (RMG-II and JHOC-8) had a Met/hTERT ratio greater than 1.5.
doi:10.1371/journal.pone.0057724.g004

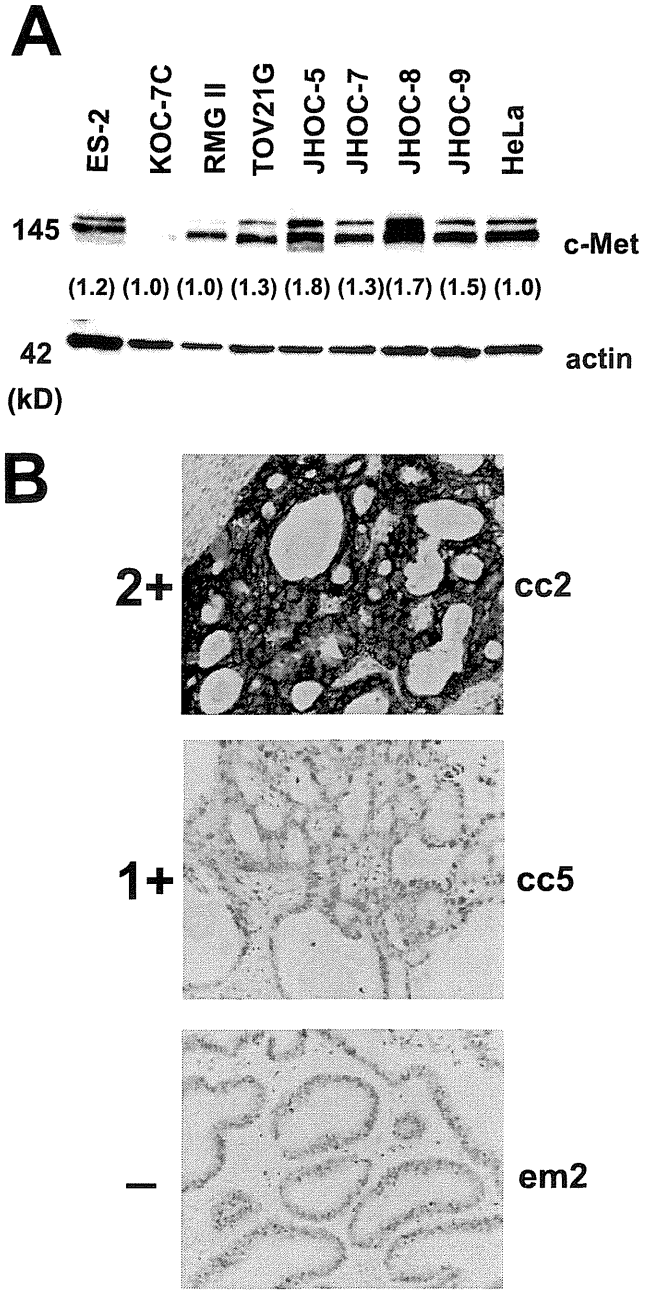

Figure 5. Confirmation of Met amplification at the protein level. A. The immunoblotting results for Met protein expression in ovarian clear cell adenocarcinoma cell lines. Two cell lines (JHOC-5 and JHOC-8) with Met gene amplification show stronger intensities. **B.** The immunostaining results of representative cases (cc2, Met-amplified ovarian clear cell adenocarcinoma (OCC) case; cc5, OCC case without Met amplification; em2, endometrioid adenocarcinoma case without Met amplification). Positive staining for c-Met antibody was further divided to 2 groups: 2+ and 1+ (see text for details).
doi:10.1371/journal.pone.0057724.g005

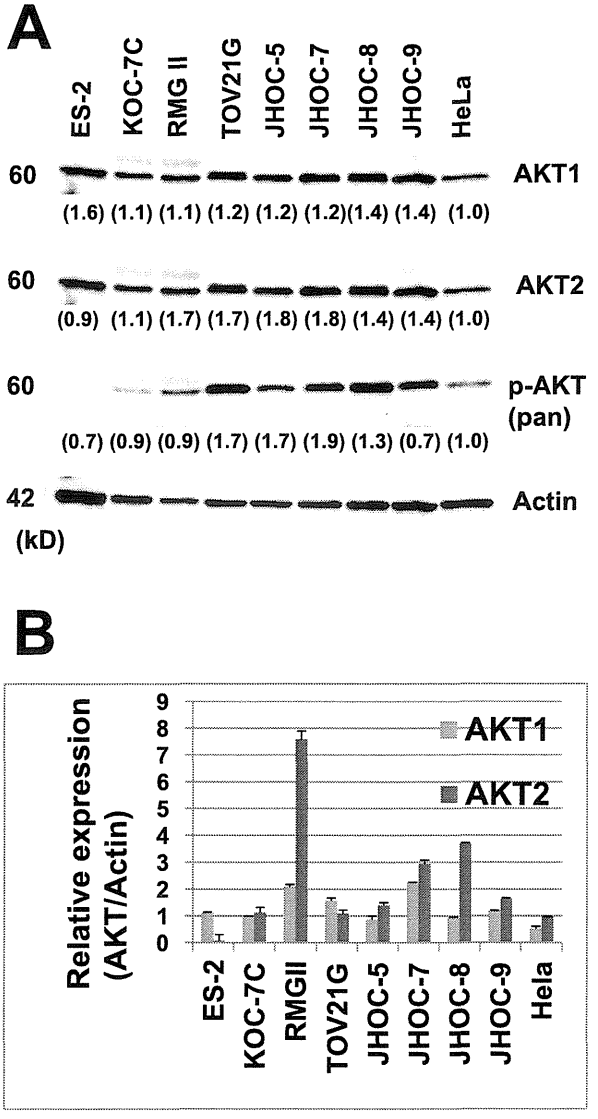

Figure 6. AKT1 and AKT2 expression in ovarian clear cell adenocarcinoma. A. Western blot analyses of protein expression using AKT antibodies in ovarian clear cell adenocarcinoma cell lines. Various intensities are observed by immunoblotting with AKT1, AKT2, and pan-AKT phosphorylated antibodies (serine 473 phosphorylated-AKT). **B.** A qRT-PCR analysis revealed relatively higher expression of AKT2 compared to AKT1 at the mRNA level.
doi:10.1371/journal.pone.0057724.g006

most OCC cells compared with HeLa cells, and immunoblotting using a phosphorylated-AKT (Ser473) antibody that recognizes the activated forms of all three isoforms of AKT was positive in all OCC cell lines showing AKT activation (**Fig. 6A**). To compare the relative amount of AKT isoform expression, we further performed a qRT-PCR analysis based on standard curves using plasmids encoding the PCR amplicons of AKT1 and AKT2, which were similar in length, as templates for the corresponding PCR. Interestingly, higher expression of AKT2 was observed in most OCC cell lines compared with AKT1 (**Fig. 6B**).

Met Amplification and Overall Survival

A qPCR analysis revealed that 27 of the 73 cases had a greater than 2-fold increase in Met gene expression (37.0%). Similarly, 19 of the 53 (35.9%) stage 1 & 2 patients had Met amplification, and these patients had significantly worse overall survival compared with patients without Met amplification ($p = 0.037$) (**Fig. 7**). We then analyzed 73 OCC samples to calculate the exact rate of AKT2 amplification. However, in total, only 6 of the 73 cases had a greater than 2-fold increase in AKT2 gene expression (8.2%) by qPCR, and no significant difference in survival was detected. We therefore focused on Met in further analyses.

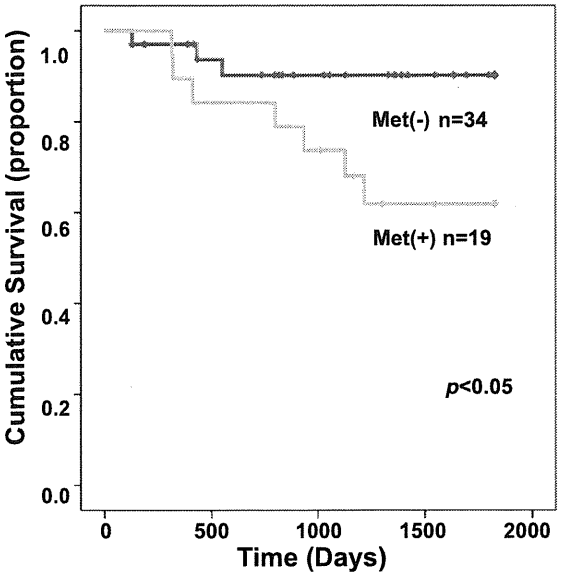

Figure 7. The Kaplan-Meier curve of stage 1 and 2 ovarian clear cell adenocarcinoma patients with or without Met amplification. Patients with Met amplification had a significantly worse prognosis ($p<0.05$).
doi:10.1371/journal.pone.0057724.g007

Met Knockdown Experiments *in vitro*

Met knockdown resulted in a large decline of cell proliferation and survival in Met-amplified OCC cell lines (**Fig. 8**). We confirmed Met knockdown at the protein level by Western blotting (**Fig. 8A**). Met knockdown in JHOC-5 and JHOC-8 cells by two independent shRNAs resulted in a significant decrease in the number of viable cells in the MTT assay compared with control shRNA (**Fig. 8B**). This was further confirmed to be the result of significantly larger numbers of cells undergoing apoptosis in OCC cell lines, and positive senescence marker staining only in Met-amplified OCC cell lines; JHOC-5 and JHOC-8 (**Fig. 8C**), suggesting that an active Met pathway was necessary for both cell survival and proliferation. Met knockdown in ES-2 cells, an OCC cell line without Met amplification, showed a partially significant decrease in cell numbers by the cell viability assay using MTT assay compared with control shRNA (**Fig. 8B**), and this was mostly due to increased apoptosis in these cells (**Fig. 8C**). Met knockdown in HeLa cells did not have a significant impact on the results of the MTT, TUNEL, and senescence assays (**Fig. 8**).

Discussion

In this study, we successfully detected Met amplification by array-based CGH analysis in 6 of the 21 OCC samples, and the final amplification rate was 37.0% when 73 cases were evaluated. Using similar methods, previous studies have not detected such frequent amplification of a specific gene. The reason for the discrepancy remains unclear. However, we used DNA extracted from paraffin sections, in which estimation of the tumor proportion by histological analyses is easier, and DNA was extracted from regions with a tumor proportion greater than 70%. Regional and ethnic differences of the patients may have also played a role. Yamamoto et al reported Met amplification in 28% of Japanese OCC cases [13], and Rhaman et al demonstrated that ZNF217 at chromosome 20q13.2 was amplified in 20% of their OCC patients [14]. Our array-based CGH data also showed rather frequent amplification of various genes (**Table S1**), but Met was the most frequently amplified, confirming Yamamoto's findings. We also demonstrated the frequent amplification of AKT2, which was identified in 5/21 samples using array-based CGH analysis and 7.5% of the 73 OCC samples using qPCR. Our array-based CGH data also revealed ZNF217 amplification in 2 cell lines (RMG-II and JHOC-9) and Her2 amplification in one cell line (RMG-II) (**Fig. S2**), but neither gene was included in **Table S1** because of the lower frequency. Most recently, Yamamoto et al also reported amplification of actinin 4 at chromosome 19 13.2 [18]. Although several genes at this region were included in our list (**Table S1**), actinin 4 was also not significantly amplified in our cases. In addition, our OCC cases were primarily associated with endometriosis, which is typically prominent in Japanese cases [1,19] and was histologically confirmed in the majority of our cases (**Table 1**). Thus, the association with endometriosis may have been related to the frequency of gene amplification. We further confirmed Met amplification using various methods such as qPCR, immunoblotting, and immunohistochemistry. All of these results showed good correlation, and we therefore suggest that Met amplification may be one of the key molecular events in OCC development, particularly in Japanese cases. Most recently, we reported that Met amplification was frequently observed in the tumor samples of an Fe-NTA-induced rat renal carcinogenesis model [4]. We propose that oxidative stress due to excess iron deposition is the primary cause of carcinogenesis in endometriosis-associated ovarian clear cell carcinomas [2,20]. It is then interesting that a key molecular event, Met amplification, is commonly observed in both human OCC and the Fe-NTA-induced animal model. This emphasizes the importance of an underlying biological and molecular mechanism of iron-induced carcinogenesis.

In this study, we also observed amplification of AKT2, one of the three isoforms of the AKT kinase family [21]. Although previously reported in ovarian serous neoplasms [22], our study is the first to report AKT2 amplification in clear cell adenocarcinoma. PI3K is one of the downstream effectors recently shown to be mutated in more than 30% of OCC cases [6]. AKT is a further downstream component of the Met/PI3K signaling pathway [23]. Considered alongside our data, this suggests that activation of the Met/PI3K/AKT2 pathway may have an important role in OCC carcinogenesis. mTOR, another component of the Met/PI3K/AKT2 pathway downstream of PI3K, inhibits p53 via increased Mdm2 translation [24], and p53 is known to induce both apoptosis and senescence [25]. Because Met knockdown in OCC cell lines with Met amplification showed both increased apoptosis and senescence *in vitro* (**Fig. 8**), we believe that Met-amplified OCC cells primarily depend on activation of the Met/PI3K/AKT pathway for cell proliferation and survival.

Met gene amplification was first reported in a gastric carcinoma cell line [26], followed by a proportion of gastric and esophageal adenocarcinomas [27–29], non-small cell carcinoma of the lung [30,31], colorectal adenocarcinoma [32], and squamous cell carcinoma of the head and neck [33]. Met amplification is usually accompanied by overexpression of the Met protein [34], and studies have been conducted to elucidate the biological significance of Met overexpression with or without amplification, with mostly similar conclusions: tumors with Met overexpression have a worse prognosis [30,34–39]. Furthermore, recent reports have proposed that the growth and survival of Met-amplified tumor cells are fully dependent on Met and explained this as an example of 'oncogene addiction' [40,41]. In our study, OCC cell lines with Met amplification were significantly dependent on Met for cell growth and survival. We therefore believe that OCC tumor cells are also 'addicted' to Met. Previous studies have demonstrated

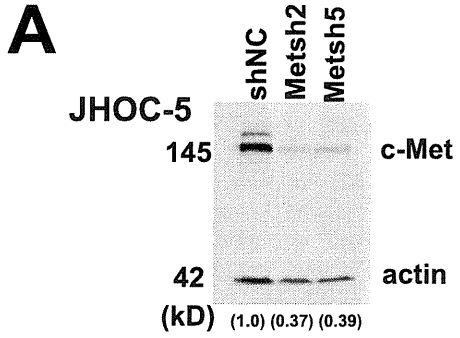

Relative intensity (Metsh/shNC)

	JHOC-5	JHOC-8	ES-2	Hela
shNC	1	1	1	1
Metsh2	0.37	0.43	0.33	0.49
Metsh5	0.39	0.32	0.37	0.51

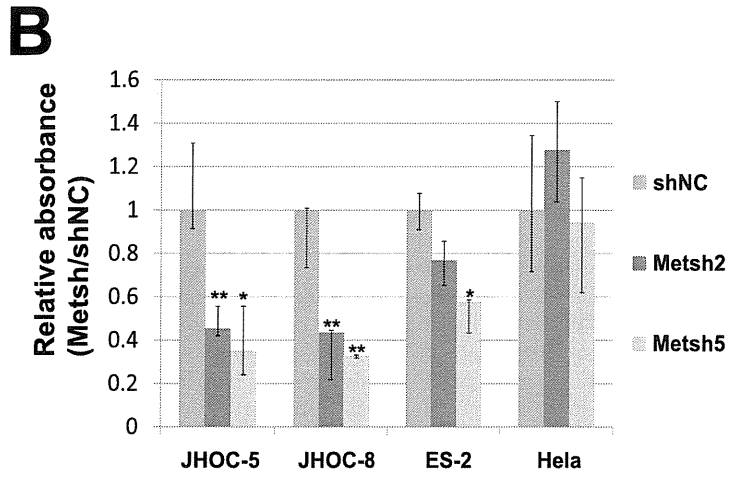

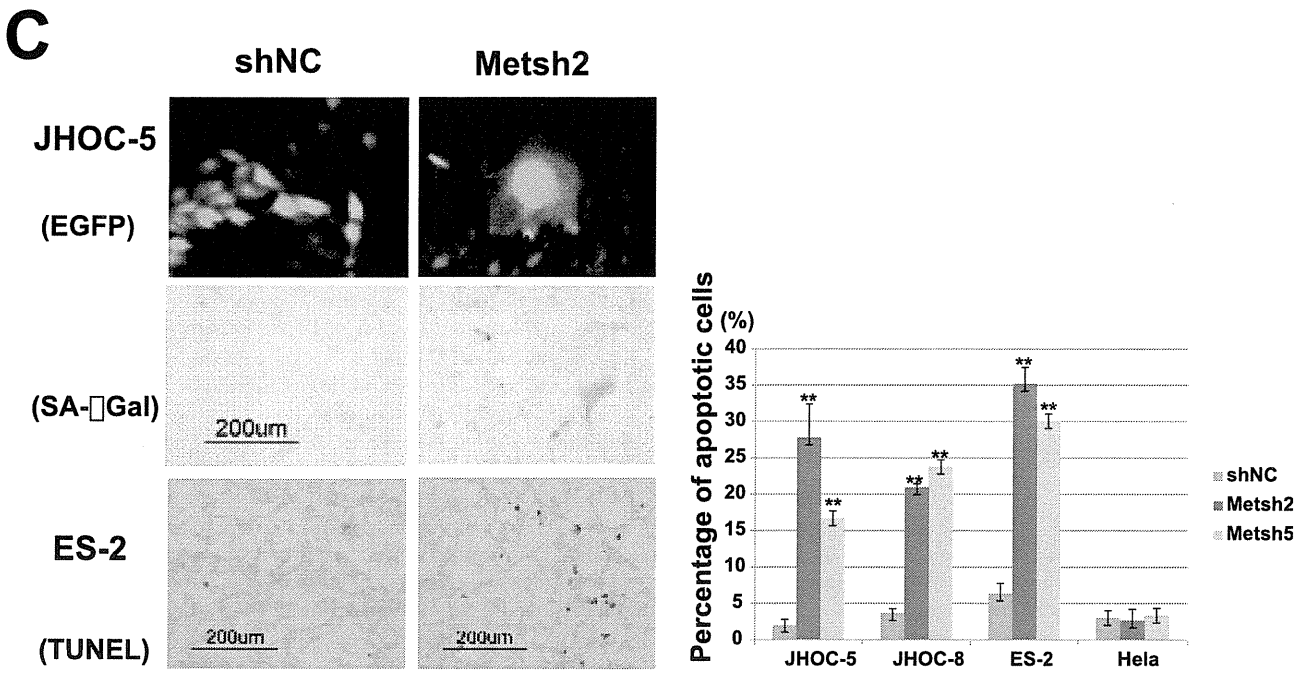

Figure 8. Knockdown of Met in ovarian clear cell adenocarcinoma cell lines. A. Confirmation of knockdown by Western blotting. Signal intensity ratio (Met/actin) are shown in numbers. B. Cell viability assay after transfection using retroviral vectors encoding short-hairpin RNAs targeting Met (Metsh2 and Metsh5) or control, shNC, in ovarian clear cell adenocarcinoma (OCC) cell lines. A decrease in cell viability in OCC cell lines with Met amplification (JHOC-5 and JHOC-8) is evident compared to ES-2 (OCC cell without Met amplification) or control HeLa cells. *$p<0.05$, ** $p<0.01$ **C.** Morphologically, Met-amplified cells (JHOC-5) expressing Metsh and enhanced green fluorescent protein (EGFP) became larger and were positively stained with SA-βGal (a senescence marker) compared with control. The number of apoptotic cells with nuclear staining in TdT-mediated dUTP-biotin nick end labeling (TUNEL) assay also significantly increased as a result of Met knockdown in cells with Met amplification (JHOC-5 and JHOC-8) or without Met amplification (ES-2), compared with controls.
doi:10.1371/journal.pone.0057724.g008

inactivation of the Met pathway by specific small inhibitors [42,43], which are particularly effective in the treatment of 'Met oncogene-addicted' carcinomas [40], and we suggest that OCC is another optimal target for Met-targeting therapies.

In conclusion, we demonstrated frequent genomic amplification of the Met gene by comprehensively analyzing the total genome, showing that Met was the most frequently amplified gene in Japanese OCC samples. Furthermore, we also detected the amplification of AKT2, which is a downstream component of the Met/PI3K signaling pathway. Targeted therapy inhibiting the Met/PI3K/AKT pathway may be promising for OCC treatment.

Supporting Information

Figure S1 Frequency distribution result of genomic alterations in each chromosome of array-based comparative genome hybridization analysis. Relative frequencies of genomic loss (green bar) and gain (red bar) for 13 primary ovarian clear cell adenocarcinoma tissue samples are plotted at each chromosomal position. Regions of genomic alteration in a single profile were identified using the Z-score statistical algorithm.
(PDF)

Figure S2 Gene views of chromosomes 20 and 17 of the genomic changes observed by array-based CGH analysis in the 21 ovarian clear cell adenocarcinoma samples. Low peaks within 1 Mb are observed in 2/21 samples at the genomic region encoding ZNF217 (upper row). The amplified region including Her2 is also shown (lower row).
(PDF)

Table S1 Frequently amplified regions of the chromosome and included genes detected by array-based comparative genomic hybridization.
(XLSX)

Acknowledgments

The authors thank Ms. Y Tanaka and Mr. N Misawa for their excellent technical assistance.

Author Contributions

Conceived and designed the experiments: Y. Yamashita ST. Performed the experiments: Y. Yamashita KS H. Kobayashi HS. Analyzed the data: Y. Yamashita SA. Contributed reagents/materials/analysis tools: Y. Yatabe H. Kajiyama FK TT. Wrote the paper: Y. Yamashita.

References

1. Mandai M, Yamaguchi K, Matsumura N, Baba T, Konishi I (2009) Ovarian cancer in endometriosis: molecular biology, pathology, and clinical management. Int J Clin Oncol 14: 383–391.
2. Yamaguchi K, Mandai M, Toyokuni S, Hamanishi J, Higuchi T, et al. (2008) Contents of endometriotic cysts, especially the high concentration of free iron, are a possible cause of carcinogenesis in the cysts through the iron-induced persistent oxidative stress. Clin Cancer Res 14: 32–40.
3. Liu YT, Shang D, Akatsuka S, Ohara H, Dutta KK, et al. (2007) Chronic oxidative stress causes amplification and overexpression of ptprz1 protein tyrosine phosphatase to activate beta-catenin pathway. American J Pathol 171: 1978–1988.
4. Akatsuka S, Yamashita Y, Ohara H, Liu YT, Izumiya M, et al. (2012) Fenton Reaction Induced Cancer in Wild Type Rats Recapitulates Genomic Alterations Observed in Human Cancer. PLoS One 7 e43403.
5. Itamochi H, Kigawa J, Terakawa N (2008) Mechanisms of chemoresistance and poor prognosis in ovarian clear cell carcinoma. Cancer Sci 99: 653–658.
6. Kuo KT, Mao TL, Jones S, Veras E, Ayhan A, et al. (2009) Frequent Activating Mutations of PIK3CA in Ovarian Clear Cell Carcinoma. Am J Pathol174: 1597–1601.
7. Jones S, Wang TL, Shih IM, Mao TL, Nakayama K, et al. (2010) Frequent Mutations of Chromatin Remodeling Gene ARID1A in Ovarian Clear Cell Carcinoma. Science 330: 228–231.
8. Wiegand KC, Shah SP, Al-Agha OM, Zhao YJ, Tse K, et al. (2010) ARID1A Mutations in Endometriosis-Associated Ovarian Carcinomas. New Eng J Med363: 1532–1543.
9. Kuo KT, Mao TL, Chen X, Feng YJ, Nakayama K, et al. (2010) DNA Copy Numbers Profiles in Affinity-Purified Ovarian Clear Cell Carcinoma. Clin Cancer Res 16: 1997–2008.
10. Dent J, Hall GD, Wilkinson N, Perren TJ, Richmond I, et al. (2003) Cytogenetic alterations in ovarian clear cell carcinoma detected by comparative genomic hybridisation. Brit J Cancer 88: 1578–1583.
11. Suehiro Y, Sakamoto M, Umayahara K, Iwabuchi H, Sakamoto H, et al. (2000) Genetic aberrations detected by comparative genomic hybridization in ovarian clear cell adenocarcinomas. Oncology 59: 50–56.
12. Tan DSP, Iravani M, McCluggage WG, Lambros MBK, Milanezi F, et al. (2011) Genomic Analysis Reveals the Molecular Heterogeneity of Ovarian Clear Cell Carcinomas. Clin Cancer Res 17: 1521–1534.
13. Yamamoto S, Tsuda H, Miyai K, Takano M, Tamai S, et al. (2011) Gene amplification and protein overexpression of MET are common events in ovarian clear-cell adenocarcinoma: their roles in tumor progression and prognostication of the patient. Mod Pathol 24: 1146–1155.
14. Rahman MT, Nakayama K, Rahman M, Nakayama N, Ishikawa M, et al. (2012) Prognostic and therapeutic impact of the chromosome 20q13.2 ZNF217 locus amplification in ovarian clear cell carcinoma. Cancer 118: 2846–2857.
15. Yamashita Y, Tsurumi T, Mori N, Kiyono T (2006) Immortalization of Epstein-Barr virus-negative human B lymphocytes with minimal chromosomal instability. Pathol Int 56: 659–667.
16. Hu Q, Akatsuka S, Yamashita Y, Ohara H, Nagai H, et al. (2010) Homozygous deletion of CDKN2A/2B is a hallmark of iron-induced high-grade rat mesothelioma. Lab Invest 90: 360–373.
17. Yamashita Y, Kajiura D, Tang L, Hasegawa Y, Kinoshita T, et al. (2011) XCR1 Expression and Biased V-H Gene Usage Are Distinct Feautres of Diffuse Large B-Cell Lymphoma Initially Manifesting in the Bone Marrow. Am J Clin Pathol 135: 556–564.
18. Yamamoto S, Tsuda H, Honda K, Takano M, Tamai S, et al. (2011) ACTN4 gene amplification and actinin-4 protein overexpression drive tumour development and histological progression in a high-grade subset of ovarian clear-cell adenocarcinomas. Histopathology 60: 1073–1083.
19. Ogawa S, Kaku T, Amada S, Kobayashi H, Hirakawa T, et al. (2000) Ovarian endometriosis associated with ovarian carcinoma: A clinicopathological and immunohistochemical study. Gynecol Oncol 77: 298–304.
20. Toyokuni S (2009) Role of iron in carcinogenesis: Cancer as a ferrotoxic disease. Cancer Sci 100: 9–16.
21. Gonzalez E, McGraw TE (2009) The Akt kinases Isoform specificity in metabolism and cancer. Cell Cycle 8: 2502–2508.
22. Nakayama K, Nakayama N, Kurman RL, Cope L, Pohl G, et al. (2006) Sequence mutations and amplification of PIK3CA and AKT2 genes in purified ovarian serous neoplasms. Cancer Biol Ther 5: 779–785.
23. Xiao GH, Jeffers M, Bellacosa A, Mitsuuchi Y, Vande Woude GF, et al. (2001) Anti-apoptotic signaling by hepatocyte growth factor/Met via the phosphatidylinositol 3-kinase/Akt and mitogen-activated protein kinase pathways. Proc Nat Acad Sci U.S.A. 98: 247–252.
24. Moumen A, Patane S, Porras A, Dono R, Maina F (2007) Met acts on Mdm2 via mTOR to signal cell survival during development. Development 134: 1443–1451.
25. Zuckerman V, Wolyniec K, Sionov RV, Haupt S, Haupt Y (2009) Tumour suppression by p53: the importance of apoptosis and cellular senescence. J Pathol 219: 3–15.
26. Giordano S, Ponzetto C, Direnzo MF, Cooper CS, Comoglio PM (1989) Tyrosine Kinase Receptor Indistinguishable from the C-Met Protein. Nature 339: 155–156.
27. Houldsworth J, Cordoncardo C, Ladanyi M, Kelsen DP, Chaganti RSK (1990) Gene Amplification in Gastric and Esophageal Adenocarcinomas. Cancer Res 50: 6417–6422.
28. Kuniyasu H, Yasui W, Kitadai Y, Yokozaki H, Ito H, et al. (1992) Frequent Amplification of the C-Met Gene in Scirrhous Type Stomach-Cancer. Biochem Biophys Res Comm 189: 227–232.
29. Miller CT, Lin L, Casper AM, Lim J, Thomas DG, et al. (2006) Genomic amplification of MET with boundaries within fragile site FRA7G and upregulation of MET pathways in esophageal adenocarcinoma. Oncogene 25: 409–418.
30. Cappuzzo F, Marchetti A, Skokan M, Rossi E, Gajapathy S, et al. (2009) Increased MET Gene Copy Number Negatively Affects Survival of Surgically Resected Non-Small-Cell Lung Cancer Patients. J Clin Oncol 27: 1667–1674.
31. Turke AB, Zejnullahu K, Wu YL, Song Y, Dias-Santagata D, et al. (2010) Preexistence and Clonal Selection of MET Amplification in EGFR Mutant NSCLC. Cancer Cell 17: 77–88.
32. Direnzo MF, Olivero M, Giacomini A, Porte H, Chastre E, et al. (1995) Overexpression and Amplification of the Met/Hgf Receptor Gene During the Progression of Colorectal-Cancer. Clin Cancer Res 1: 147–154.
33. Seiwert TY, Jagadeeswaran R, Faoro L, Janamanchi V, Nallasura V, et al. (2009) The MET Receptor Tyrosine Kinase Is a Potential Novel Therapeutic Target for Head and Neck Squamous Cell Carcinoma. Cancer Res 69: 3021–3031.

34. Nakajima M, Sawada H, Yamada Y, Watanabe A, Tatsumi M, et al. (1999) The prognostic significance of amplification and overexpression of c-met and c-erb B-2 in human gastric carcinomas. Cancer 85: 1894–1902.
35. Nakazawa K, Dobashi Y, Suzuki S, Fujii H, Takeda Y, et al. (2005) Amplification and overexpression of c-erbB-2, epidermal growth factor receptor, and c-met in biliary tract cancers. J Pathol 206: 356–365.
36. Sawada K, Radjabi AR, Shinomiya N, Kistner E, Kenny H, et al. (2007) c-Met overexpression is a prognostic factor in ovarian cancer and an effective target for inhibition of peritoneal dissemination and invasion. Cancer Res 67: 1670–1679.
37. Ghoussoub RAD, Dillon DA, D'Aquila T, Rimm EB, Fearon ER, et al. (1998) Expression of c-met is a strong independent prognostic factor in breast carcinoma. Cancer 82: 1513–1520.
38. Kaposi-Novak P, Lee JS, Gomez-Quiroz L, Coulouarn C, Factor VM, et al. (2006) Met-regulated expression signature defines a subset of human hepatocellular carcinomas with poor prognosis and aggressive phenotype. J Clin Invest116: 1582–1595.
39. Lo Muzio L, Farina A, Rubini C, Coccia E, Capogreco M, et al. (2006) Effect of c-Met expression on survival in head and neck squamous cell carcinoma. Tumor Biol 27: 115–121.
40. Smolen GA, Sordella R, Muir B, Mohapatra G, Barmettler A, et al. (2006) Amplification of MET may identify a subset of cancers with extreme sensitivity to the selective tyrosine kinase inhibitor PHA-665752. Proc Nat Acad Sci U.S.A. 103: 2316–2321.
41. Bachleitner-Hofmann T, Sun MY, Chen CT, Tang L, Song L, et al. (2008) HER kinase activation confers resistance to MET tyrosine kinase inhibition in MET oncogene-addicted gastric cancer cells. Mol Cancer Ther 7: 3499–3508.
42. Christensen JG, Schreck R, Burrows J, Kuruganti P, Chan E, et al. (2003) A selective small molecule inhibitor of c-Met kinase inhibits c-Met-dependent phenotypes in vitro and exhibits cytoreductive antitumor activity in vivo. Cancer Res 63: 7345–7355.
43. Koon EC, Ma PC, Salgia R, Welch WR, Christensen JG, et al. (2008) Effect of a c-Met-specific, ATP-competitive small-molecule inhibitor SU11274 on human ovarian carcinoma cell growth, motility, and invasion. Int J Gynecol Cancer 18: 976–984.